HHS Public Access

Author manuscript

Nature. Author manuscript; available in PMC 2015 January 17.

Published in final edited form as:

Nature. 2014 July 17; 511(7509): 312–318. doi:10.1038/nature13547.

Reprogramming Human Endothelial to Hematopoietic Cells Requires Vascular Induction

Vladislav M. Sandler[1], **Raphael Lis**[1], **Ying Liu**[1], **Alon Kedem**[1,2], **Daylon James**[1,2], **Olivier Elemento**[3], **Jason M. Butler**[1], **Joseph M. Scandura**[4], and **Shahin Rafii**[1]

[1]Ansary Stem Cell Institute, Department of Genetic Medicine, and Howard Hughes Medical Institute, Weill Cornell Medical College, New York, NY 10065

[2]Ronald O. Perelman and Claudia Cohen Center for Reproductive Medicine, Weill Cornell Medical College, New York, NY 10065

[3]HRH Prince Alwaleed Bin Talal Bin Abdulaziz Alsaud Institute for Computational Biomedicine, Weill Cornell Medical College, New York, NY, 10065

[4]Department of Medicine, Hematology-Oncology, Weill Cornell Medical College and the New York Presbyterian Hospital, New York, NY, 10065

Summary

Generating engraftable human hematopoietic cells from autologous tissues promises new therapies for blood diseases. Directed differentiation of pluripotent stem cells yields hematopoietic cells that poorly engraft. Here, we devised a method to phenocopy the vascular-niche microenvironment of hemogenic cells, thereby enabling reprogramming of human endothelial cells (ECs) into engraftable hematopoietic cells without transition through a pluripotent intermediate. Highly purified non-hemogenic human umbilical vein-ECs (HUVECs) or adult dermal microvascular ECs (hDMECs) were transduced with transcription factors (TFs), *FOSB*, *GFI1*, *RUNX1*, and *SPI1* (FGRS), and then propagated on serum-free instructive vascular niche monolayers to induce outgrowth of hematopoietic colonies containing cells with functional and immunophenotypic features of multipotent progenitor cells (MPP). These reprogrammed ECs- into human-MPPs (rEC-hMPPs) acquire colony-forming cell (CFC) potential and durably engraft in immune-deficient mice after primary and secondary transplantation, producing long-term rEC-hMPP-derived myeloid (granulocytic/monocytic, erythroid, megakaryocytic) and lymphoid (NK, B) progeny. Conditional expression of FGRS transgenes, combined with vascular-induction, activates endogenous FGRS genes endowing rEC-hMPPs with a transcriptional and functional profile similar to self-renewing MPPs. Our approach underscores the role of inductive cues from vascular-niche in orchestrating and sustaining hematopoietic specification and may prove useful for engineering autologous hematopoietic grafts to treat inherited and acquired blood disorders.

Contributions

V.M.S. and S.R. conceived and designed the project, performed experiments, analyzed the data and wrote the manuscript. R.L., Y.L., and J.M.B. performed experiments interpreted, and analyzed data. J.M.S. interpreted, analyzed data and wrote the manuscript. D.J., O.E., A.K., performed the experiments and analyzed the data. All authors commented on the paper.

Manufacture of autologous engraftable hematopoietic stem and progenitor cells (HSPC) offers tremendous therapeutic potential. Using *in vitro* cultures, human pluripotent stem cells can be differentiated into hematopoietic progenitors, which often have limited expansion potential and do not engraft myeloablated recipients[1–3]. Enforced expression of transcription factors (TFs) has also been used to reprogram somatic cells, into hematopoietic lineages[4–6]. Employing cellular fusion, we have shown that direct conversion of somatic cells into fetal HSPCs is also feasible[7]. Yet, these prior efforts have been unable to produce human hematopoietic cells capable of long-term multilineage engraftment[4–7]. We hypothesized that in addition to TF expression, hematopoietic specification and long-term engraftment may require inductive signals from the microenvironment. Indeed, the central instructive role of tissue-specific endothelial cells (EC)[8]in supporting organ regeneration[9,10], including hematopoietic stem cell (HSC) self-renewal and reconstitution of multilineage hematopoiesis, has recently come to light[11–18].

In mammals, definitive HSCs originate in the vascular microenvironment of the aorta-gonad-mesonephros (AGM)[19–24], placenta[25] and arterial vessels[26]. Putative HSCs bud off from hemogenic vascular cells lining the dorsal aorta floor and umbilical arteries, where they are in cellular contact with non-hemogenic ECs[27]. This ontological endothelial to hematopoietic transition (EHT) is mediated in part through expression of the TF RUNX1[21], its non-DNA binding partner core binding factor-β[28], GFI1 and GFI1b[29,30]. However, the contribution of micro-environmental inductive signals provided by anatomically distinct niches and tissue-specific vascular niches[8] within the AGM, fetal liver and placenta remain poorly defined.

We have identified a minimal set of four TFs—*FOSB, GFI1*, *RUNX1*, and *SPI1* (FGRS)—that reprogram full-term human umbilical vein ECs (HUVECs) and human adult dermal microvascular ECs (hDMEC) into hematopoietic cells with long-term multipotent progenitor cell (MPP) activity (rEC-hMPP). The reprograming was successful only when a unique serum-free vascular niche platform was used. Subsets of rEC-hMPPs were immunophenotypically marked as HSCs and were capable of long-term primary and secondary multilineage engraftment in immunodeficient mice. We demonstrate that enforced or transient expression of FGRS-TFs combined with inductive signals from specialized vascular niche Calls[1,11,31] are essential for efficient conversion of ECs into rEC-hMPPs.

Results

FGRS-TFs and vascular-induction reprogramming

Primitive HSCs emerge on a vascular bed during development. Thus, we hypothesized that the vascular niche could play an important role during reprogramming by inducing and maintaining nascent hematopoietic cells. Since serum impairs vascular function and interferes with expansion of HSCs and MPPs, we devised a vascular niche model, in which ECs transduced with the adenoviral *E4ORF1* gene (E4ECs, VeraVecs) could be cultured without serum[1,11,12,31]. E4ORF1 activates survival pathways in ECs without provoking proliferation or cellular transformation and thereby maintain tissue-specific functional and metabolic attributes of ECs. E4ECs-derived from HUVECs[1,11,12,31] or ECs purified and

propagated from hematopoietic organs[32,33] balance self-renewal and differentiation of human and mouse long-term HSCs and MPPs by production of physiological levels of Notch-ligands, Kit-ligand, BMPs, Wnts and other angiocrine factors[14].

To identify TFs that drive EHT, we first identified TFs differentially expressed by $Lin^{-}CD34^{+}$ umbilical cord HSPCs, but not by HUVECs (Extended Data Figure 1A–D). We then cultivated $CD45^{-}CD133^{-}cKit^{-}$ $CD31^{+}$ HUVECs that were devoid of hemogenic potential[34] (Figure 1A) and transduced them with lentiviral-vectors expressing various combinations of differentially-expressed TF transcripts using GFP as a marker. Three days after transduction, HUVECs were replated on subconfluent serum-free E4EC-monolayers. Within2 weeks of co-culture with E4ECs, round $GFP^{+}CD45^{+}$ cells began to bud from transduced HUVECs and morph into grape-like colonies (Figure 1B). Systematic one-by-one dropout of candidate TFs demonstrated that expression of *FOSB*, *GFI1*, *RUNX1*, and *SPI1* (FGRS) was necessary and sufficient for hematopoietic reprogramming of HUVECs (Extended Data Figure 1B, C). Co-culture of FGRS transduced-ECs (FGRS-EC) with E4EC monolayers augmented the yield and stability of the hematopoietic-like colonies, which manifested morphological features of hematopoietic progenitors (Figure 1C). Within 4 weeks of co-culture with E4ECs, FGRS-ECs began to proliferate and form $GFP^{+}CD45^{+}$ colonies (Figure 1A,C). Serum suppressed colony formation and naïve HUVECs could not survive without serum and failed to support the emergence of $CD45^{+}$cells (Figure 1D). FGRS-transduction of 5×10^{4} HUVECs followed by 3-weeks of serum-free co-culture with E4ECs yielded 32.3±10.5 colonies (Figure 1D) (efficiency of reprogramming 1.5% see methods), occasionally forming multi-colony structures (Extended Data Figure 2A). Once colonies formed, proliferation of GFP^{+} cells increased and after 5 weeks of co-culture with E4ECs, up to 20×10^{6} $GFP^{+}CD45^{+}$ cells were produced, a ~400-fold expansion of the input FGRS-ECs (Figure 1D). Since clonal $CD45^{+}$cells, but not $CD45^{-}$ cells, form colonies it is unlikely that E4ECs are mistakenly identified as hematopoietic cells (Extended Data Figure 2B,C). Thus, FGRS-ECs required sustained inductive and supportive signals from E4EC-vascular niche for efficient hematopoietic reprogramming.

To date, efforts to differentiate pluripotent stem cells into repopulating hematopoietic cells have had limited success[1–3]. We hypothesized that FGRS-TFs could augment hematopoietic differentiation of human embryonic stem cells (hES). To test this, we first differentiated hESCs into ECs (hES-EC)[35,36] and then transduced purified $VEGFR2^{+}CD144^{+}$ hES-ECs with FGRS. Although this approach generated $CD45^{+}CD144^{-}$ progeny (Extended Data Figure 2D), these cells did not form stable hematopoietic-like colonies and did not proliferate (Figure 1A black line). Thus, hES-ECs are not as permissive as HUVECs for reprogramming into hematopoietic cells.

rEC-MPPs have features of multilineage progenitors

During reprogramming, GFP^{+} FGRS-ECs and vascular-induced hematopoietic-like colonies lost CD31, but gained the expression of hematopoietic markers CD45, CD43, CD90(Thy-1) and CD14 (Figure 2A and Extended Data Figure 2E). In contrast, the GFPE4ECs remained $CD31^{+}CD34^{+}CD45^{-}$ Importantly, a subset of $GFP^{+}CD45^{+}$FGRS-EC progeny manifested the immunophenotype of human MPPs ($CD45^{+}Lin^{-}$ $CD45RA^{-}CD38^{-}CD90^{+}CD34^{+}$) and

HSCs ($CD45^+Lin^-CD45RA^-CD38^-CD90^-CD34^+$)[37,38](Figure 2B). To assess the function of various populations of these ECs reprogrammed into human MPPs (rEC-hMPPs), we sorted four week-old $GFP^+CD45^+CD34^+$ rEC-hMPPs and seeded them in colony-forming cells (CFC) assays to enumerate progenitor cells. The rEC-MPPs gave rise to GFP^+ colonies with CFU-GEMM (granulocytic/erythroid/megakaryocytic/monocytic), CFU-GM (granulocytic/macrophage), and hemoglobinized BFU-E (erythroid) morphologies (Figure 2C). FACS and cytospin analysis documented presence of cells with morphological (Figure 2D) and immunophenotypic features of granulocyte/macrophage ($CD11b^+$, $CD14^+$), erythroid ($CD235^+$), dendritic ($CD83^+$) and megakaryocyte ($CD41a^+$) progenies (Extended Data Figure 2F). The function of rEC-hMPP-derived macrophages was corroborated using a phagocytosis assay (Extended Data Figure 2G). Thus, rEC-hMPPs contain functional multilineage progenitor cells.

rEC-hMPPs engraft long-term into primary recipients

To assess the engraftment potential of rEC-hMPPs, we transplanted 1.5×106 $CD45^+GFP^+$rEC-hMPPs into adult sub-lethally irradiated (275 Rad) immunocompromised-NSG mice (Figure 3A). We detected circulating human $CD45^+$ cells in the peripheral blood (PB) of recipient engrafted mice from 2 to 44 weeks (Figure 3B) and found $CD45^-CD235^+$ erythroid cells 16 weeks, post-transplantation (Figure 3C). We then sorted $hCD45^+$ cells from bone marrow (BM) of recipient mice 22 to 24 weeks after transplantation and cultured them for 24 hours. The $hCD45^+hCD34^+$ cells were resorted and seeded into CFC-assays. They formed CFU-GM, CFU-GEMM, and BFU-E hematopoietic colonies with typical myeloid progeny morphologies (Figure 3D). Hence, rEC-hMPPs are capable of robust multilineage engraftment.

rEC-hMPPs are derived from non-hemogenic ECs

To rule out the possibility that rEC-hMPPs are derived from rare contaminating hemogenic cells[25,34], we cultured naïve ECs in optimal pro-hematopoietic media or performed clonal reprogramming of ECs. Neither serum-withdrawal, nor addition of hematopoietic cytokines induced formation of $CD45^+CD34^+$cells from naïve HUVECs (Extended Data Figure 3A,B). Furthermore, clonal cultures of mature $CD45^-CD144^+CD31^+CD62E(E\text{-selectin})^+$ ECs[32,33] did not form $CD45^+$rEC-MPPs (Extended Data Figure 3C,D and Extended Data Figure 4A,B,C). Thus, rEC-hMPPs were not derived from scarce population of spontaneously differentiating ECs with preexisting hemogenic potential.

The BM of robustly engrafted recipient NSG mice contained a small population of cells with $Lin^-CD45RA^-CD38^-CD90^-CD34^+$ immunophenotype of human MPPs[37] (Figure 3E). To ensure that engrafted cells were derived from FGRS-ECs, we purified $hCD45^+$ cells from recipient BM (Figure 3F) and seeded single-cells into 96-well plates for whole genome amplification (WGA) and detection of viral vector integration. All $hCD45^+$ cells had been transduced by lentiviral vectors, and 19/21 cells showed integration of all four FGRS-TFs (Figure 3F, Extended Data Figure 5). To verify that these cells were progeny of rEC-hMPPs, we seeded $hCD45^+$ cells for CFC-assays to examine viral integration in individual colonies (Figure 3G). We demonstrated that all tested colonies were derived from cells that had

integrated the lentiviral vectors expressing *FGRS* (Figure 3G). Therefore, engrafted human hematopoietic cells were derived from transplanted rEC-hMPPs.

To test whether FGRS-induced reprogramming triggered expression of endogenous human FGRS genes[24], we expressed genetically distinct murine TFs (mFGRS) using inducible-lentiviral vectors to reprogram HUVECs into rEC-hMPPs and then assessed for endogenous human FGRS-gene expression. Transient expression of mFGRS with E4EC-coculture for 3-weeks induced a 100-fold greater expression of endogenous genes than that of switched-off mFGRS transcripts (Extended Data Figure 6A,B,C). Therefore, rEC-hMPPs do not require continuous expression of exogenous FGRS-TFs to sustain their hematopoietic cell fates.

Furthermore, we speculated that enforced SPI1 expression might prevent rEC-hMPPs from differentiating into T-cells[39,40] Therefore, we constitutively expressed FGR-TFs with a Tet-inducible *SPI1* and E4EC-induction, which resulted in generation of small but significant population of $CD3^+$ T-cells (Extended Data Figure 6D,E). Thus, generation of lymphoid cells from rEC-hMPPs could be optimized by transient expression of specific TFs.

Adult ECs are reprogrammable to rEC-hMPPs

To test whether our approach could reprogram adult human ECs, we transduced hDMECs with FGRS-TFs and propagated them on serum-free E4EC-monolayers (Figure 4A). After 4 weeks $GFP^+hCD45^+CD34^+$cells were sorted for CFC-assay. The rEC-hMPPs yielded cells with morphological features of hematopoietic (Figure 4Ba) and functional myeloid CFU-GM, CFU-GEMM, and BFU-Es (Figure 4Bb), containing $CD235^+$erythroid, $CD33^+/CD14^+/CD11b^+$macrophage/monocyte, and $CD83^+$dendritic progenies (Figure 4Bb and Extended Data Figure 7A).

Next, we compared the transcription profiles of rEC-hMPPs, before and after NSG engraftment, to those of naive HUVEC, hDMEC and purified Lin-$CD34^+$ cord blood HSPCs (Figure 4C). FGRS-transduction plus E4EC-induction activated hematopoietic genes and down-regulated vascular gene signatures (Figure 4C). Importantly, 22-weeks post-transplantation, $CD45^+CD34^+$ rEC-hMPPs had a transcription pattern similar to normal $CD34^+$cord blood HSPCs and distinct from the ECs from which they were derived (Figure 4C). Notably, pluripotency genes were not induced in rEC-hMPPs indicating that reprogramming does not require transition through a destabilizing pluripotent intermediate (Figure 4D).

rEC-hMPPs engraft primary & secondary recipients

To assess engraftment potential of hDMEC-derived rEC-hMPP, we transplanted 1×10^5 $CD45^+GFP^+$rEC-hMPP into sub-lethally irradiated (100 Rads) 2-weeks old neonatal NSG mice (Figure 5A). Circulating $hCD45^+$cells were detected in the PB of recipient animals 4 (2.09±1.27%), 6 (4.46±3.66%), and 12 (4.05±3.50%) weeks post-transplantation (Figure 5A). Fourteen weeks post-transplantation, human hematopoietic cells were found in PB, BM and spleen (Figure 5A and Extended Data Figure 5B,C, D). Notably, these recipient animals harbored myeloid and lymphoid populations, including $CD19^+$ B-cells (10.13±4.98%), $CD56^+$ NK-cells (1.62±0.67%), $CD11b^+$ monocyte/macrophages (27.66±8.92%;) and

CD41a$^+$ megakaryocytes (4.90±1.51%;) in their spleens (Figure 5A and Extended Data Figure 7B,C,D). Hence, rEC-hMPPs are capable of prolonged multilineage hematopoietic engraftment. The BM of primary recipient mice (week 12–14) contained populations with the immunophenotype of human HSCs (hCD45$^+$Lin$^-$ CD45RA$^-$CD38$^-$CD90$^+$CD34$^+$, 10.37±2.55%) and MPPs ((hCD45$^+$Lin$^-$ CD45RA$^-$CD38$^-$CD90$^-$CD34$^+$, 13.83±2.14%) (Extended Figure 7D)[37,38]. Because these populations can self-renew, we tested whether BM cells of mice engrafted by primary rEC-hMPPs (12 weeks post-transplant) could engraft secondary NSG recipient mice. Indeed, the PB of secondary recipients was engrafted by human myeloid and lymphoid progenies 3(14.61±15.7%), 5(2.01±1.5%), 8(17.78±16.23%), 15(7.99±7.36%) and 23(26.3±25.7%) weeks post-transplantation (Figure 5B). Thus, subpopulations of rEC-hMPP scan self-renew and are capable of durable myeloid and lymphoid engraftment in NSG mice: characteristics similar to true hMPPs.

To examine whether individual rEC-hMPP cells retained clonal multilineage potential, we isolated hCD45$^+$hCD34$^+$cells from BM of secondarily robustly engrafted mouse 15-weeks post-transplantation and then assessed the multilineage CFC activity in clonal (1 cell/well), oligo-clonal (2 and 5 cells/well) and bulk (1000 cells/well) sorted cells (Figure 5C,D). All single-cell derived colonies displayed multilineage differentiation, including CD33$^+$/CD14$^+$/CD11b$^+$myeloid, CD41$^+$ megakaryocytic and CD235$^+$erythroid progenies (Figure 5C,D), indicating that engrafted rEC-hMPPs from secondary transplants retained their MPP potential. Thus, individual cells within the rEC-hMPPs have the immunophenotypic and functional attributes of HSPC-like/self-renewing hMPPs (Figure 5E).

Notably, rEC-hMPPs isolated from primary and secondary engrafted mice manifested no evidence of malignant transformation (Extended Data Figure 8; 9; 10A) or genetic abnormalities or (Extended Data Figure 10B).

Discussion

The availability of engraftable autologous human cells offers the potential to cure a wide spectrum of benign and malignant hematologic disorders. Prior efforts using pluripotent stem cells have been obstructed by low efficiency and poor engraftment[2,3,41,42]. Here, we have taken advantage of ontological link between endothelial and hematopoietic development to efficiently reprogram mature, fetal and adult ECs into engraftable self-renewing hMPPs without transitioning through a potentially destabilizing pluripotent intermediate. Just as support from non-hemogenic vascular cells important for EHT during development, we found the instructive contribution of the vascular niche was central to reprogramming ECs to hematopoietic cells.

Differentiating pluripotent stem cells or expanding AGM-derived cells to engraftable hematopoietic cells has been inefficient, when stromal cells have been used for niche-like support[2,3,41]. This could be due to: 1) poor inductive function of stromal cells in serum-free culture; and/or 2) distinguishing features of ECs that resemble the hematogenic niche cells that support EHT[11–15]. For example, E4ECs produce the proper stoichiometry of inductive angiocrine factors, including Notch, BMP and c-Kit pathways[4] that are important for EHT[43]. Thus, adult organ-specific pro-hematopoietic vascular niches, such as

HUVECs[11–15,36], BM[13], hepatic and splenic sinusoids[8] may share functional characteristics with EHT-inductive niche cells. The rEC-hMPPs can engraft primary and secondary recipient mice with individual cells capable of differentiating to multiple hematopoietic lineages. However, the influence of recipient microenvironmental signals and temporal aspects of reprogramming influence the outcome of xenograft studies. NSG mice lack the proper niches for T-cell differentiation and we were not able to determine whether engrafted rEC-hMPPs could give rise to T-cells. We found that temporally restricted expression of *SPI1*, along with sustained FGR, increased the ability of the rEC-hMPP to differentiate to lymphoid lineages suggesting that sustained SPI1 interfered with lymphogenesis. Notably, even transient expression of FGRS is sufficient to activate endogenous TFs. The age of recipient mice was also important because transplantation of neonatal (2-week old) NSG mice enhanced lymphoid engraftment by rEC-MPPs. Therefore, temporal and chronological expression of FGRS-TFs with proper stoichiometry combined with vascular niche signals appears to increase the yield of rEC-hMPPs with authentic multilineage long-term self-renewing HSPC potential.

Direct reprogramming of ECs into engraftable HSPCs orchestrated by the inductive signals conveyed by tissue-specific vascular niches offers an innovative way to decipher the hierarchy of TFs and micro environmental cues that guide hematopoietic development. Our approach lays a foundation for engineering engraftable autologous rEC-hMPPs and potentially true HSCs for treatment of patients with hematological disorders.

Methods Summary

Endothelial cells (ECs) were reprogrammed into hematopoietic cells by transduction with transcription factors (TFs) and vascular niche induction. To establish vascular niche-platform, ECs were purified and transduced with a lentiviral vector expressing the adenoviral *E4ORF1* gene (E4ECs, VeraVecs, Angiocrine Bioscience, NY, NY). Purified $CD45^{-}CD133^{-}cKit^{-}CD31^{+}$and clonal populations of $CD45^{-}$ $CD144^{+}CD31^{+}CD62E^{+}$ full term human umbilical vein ECs (HUVECs) and adult primary human dermal microvascular ECs (hDMEC) were cultured in EC-growth medium. Then, HUVECs or hDMECs were transduced with lentiviral vectors expressing GFP and combination of TFs: *FOSB*, *GFI1*, *RUNX1*, and *SPI1* (FGRS). After 3 days, GFP^{+} FGRS-transduced ECs were plated in co-culture with 30–50% subconfluent E4EC-monolayers supplemented with serum-free hematopoietic media composed of StemSpan SFEM, 10% KnockOut Serum Replacement, 5ng/ml FGF-2, 10ng/ml EGF, 20ng/ml SCF, 20ng/ml FLT3, 20ng/ml TPO, 20ng/ml IGF-1, 10ng/ml IGF-2, 10ng/ml IL-3 and 10ng/ml IL-6. After 3 to 4 weeks of co-culture, outgrown GFP^{+} reprogrammed ECs into human multipotent progenitor cells (rEC-hMPPs) formed typical grape-like hematopoietic colonies. After 4 weeks, human $CD45^{+}$rEC-MPPs were FACS sorted for: 1) immunophenotypic analyses, 2) methylcellulose-CFC assay, 3) molecular profiling, 4) comparative genomic hybridization and 5) transplanted retroorbitally into primary sublethally-irradiated (275 Rads) 6-week old NSG mice or sublethally-irradiated (100 Rads) 2-week old mice neonates. After three months, human $CD45^{+}$ cells ($hCD45^{+}$ cells) derived from bone marrow (BM) or whole BM of the primary engrafted mice was used for transplantation into secondary recipients. After 3 months of primary and 6 months of the secondary transplantation, engrafted $hCD45^{+}$ cells in BM, spleen and

peripheral blood of mice were FACS sorted and processed for: 1) multi-variate immunophenotypic analyses, 2) clonal and oligo-clonal CFC assay, and 3) molecular profiling. Tissues of the engrafted mice were processed for histological examination to rule out any malignant transformation.

Methods

Fetal and adult endothelial cells (ECs) used for reprogramming

Full term human umbilical vein ECs (HUVECs) were obtained as previously described[32,33]. Multiple purified populations of CD45-CD133-cKit-CD31$^+$HUVECs were isolated from separate umbilical cords (n=8) and were cultured in Endothelial Growth Media (EM): Medium 199 (Thermo Scientific: #FB-01), 20% Fetal Bovine Serum (Omega Scientific), 20 μg/ml endothelial cell supplement (Biomedical Technologies: #BT-203), 1XPen/Strep, and 20 units/ml Heparin (Sigma: # H3149-100KU). Multiple batches (n=3) of adult primary human dermal microvascular endothelial cells (hDMEC) were purchased from ScienCell Research Laboratories (cat #2020). In addition, cultured HUVECs were passaged for 3 to 5 times and then CD45$^-$ CD144$^+$ CD31$^+$ CD62E$^+$ HUVECs were sorted for clonal analyses to rule out contamination with pre-existing hemogenic ECs.

For reprogramming experiments, transduced HUVECs or hDMECs were co-cultured with E4ECs in serum-free hematopoietic media (HM) formulated as StemSpan SFEM (Stemcell Technologies), 10% KnockOut Serum Replacement (Invitrogen), 5ng/ml bFGF (FGF-2), 10ng/ml EGF, 20ng/ml SCF (soluble Kit-ligand), 20ng/ml FLT3, 20ng/ml TPO, 20ng/ml IGF-1, 10ng/ml IGF-2, 10ng/ml IL-3, 10ng/ml IL-6 (all from Invitrogen, eBioscience, or Peprotech).

Manufacturing of vascular niche platform

To establish the vascular niche monolayers, HUVECs were purified and transduced with lentiviral vector carrying a cassette of adenoviral *E4ORF1* gene (E4ECs) as previously described[31] or obtained as VeraVecs from Angiocrine Bioscience, New York, NY. E4ECs proliferate in serum-free and xenobiotic-free conditions only supplemented with minimal angiogenic factors. All naïve ECs that are non-transduced with E4ORF1 are depleted during passaging in serum-free conditions. Confluent monolayers of E4ECs are contact inhibited, non-transformed and propagate as homogenous monolayers providing ideal instructive niche for reprogramming and sustaining FGRS-transduced ECs into rEC-hMPPs.

Reprogramming of ECs into MPPs (rEC-MPPs)

ECs were reprogrammed into hematopoietic cells by transduction with transcription factors (TFs) and vascular niche induction. Purified populations of CD45$^-$CD133$^-$cKit$^-$CD31$^+$and clonal CD45$^-$ CD144$^+$CD31$^+$CD62E$^+$ full term HUVECs and adult primary hDMEC were cultured in the EC-growth medium (EM). Then, HUVECs or hDMECs were transduced with lentiviral vectors expressing GFP and combination of transcription factors (TFs), *FOSB*, *GFI1*, *RUNX1*, and *SPI1* (FGRS) and maintained in EM. After 3 days, GFP$^+$ FGRS transduced ECs were plated in co-culture with 30 to 50% subconfluent E4ECs monolayers supplemented with serum-free hematopoietic media (HM) composed of StemSpan SFEM,

10% KnockOut Serum Replacement, 5ng/ml FGF-2, 10ng/ml EGF, 20ng/ml SCF, 20ng/ml FLT3, 20ng/ml TPO, 20ng/ml IGF-1, 10ng/ml IGF-2, 10ng/ml IL-3, 10ng/ml IL-6. After 3–4 weeks of co-culture the outgrown GFP^+ reprogrammed ECs into human multipotent progenitor cells (rEC-hMPPs) formed typical grape-like hematopoietic colonies. At the end of 4 weeks, human $CD45^+$ rEC-MPPs were FACS sorted for: 1) immunophenotypic analyses, 2) methylcellulose-CFC assay, 3) molecular profiling, 4) comparative genomic hybridization and 5) transplanted retroorbitally into primary sublethally-irradiated (275 Rads) 6-week old NSG mice or sublethally-irradiated (100 Rads) 2-week old mice neonates. After three months, human $CD45^+$ cells ($hCD45^+$ cells) derived from bone marrow (BM) or whole BM of the primary engrafted mice was used for transplantation into secondary recipients. After 3 months of primary and 6 months of the secondary transplantation, engrafted $hCD45^+$ cells in BM, spleen and peripheral blood of mice were FACS sorted and processed for: 1) multi-variate immunophenotypic analyses, 2) multi-cell and clonal methylcellulose-CFC assay, and 3) molecular profiling. Tissues of the engrafted mice were processed for histological examination to rule out any malignant transformation.

Increasing Efficiency of Reprogramming

To increase efficiency of the reprogramming, we developed a strategy to select those subsets of ECs that were most likely transduced with the proper stoichiometry of all four FGRS. We initially focused on generating ECs transduced with *GFI1*, *SPI1* and *FOSB* TFs because their expression in ECs is negligible (Extended Data Fig. 1). To accomplish this, we transduced 5×10^6 ECs with FGRS lentiviral "cocktail" marked by puromycin resistance (*SPI1*) or GFP (*FOSB* and *GFI1*). We then applied puromycin selection for 2 days to enrich SPI1-expressing cells and sorted them for GFP expression to enrich for $SPI1^+GFP^+$ (*FOSB/GFI1*) ECs. Subsequently, we transduced these GFP^+ puromycin resistant cells with *RUNX1*, seeded into 12-well plates, and expanded them for two days (10^5 cells per plate, n=3). We then re-plated 10^4 of the GFP^+ puromycin resistant cells on serum-free E4EC vascular niche layer in hematopoietic media and quantified the number of hematopoietic clusters that emerge after ~20 days of co-culture. We found that GFP^+ puromycin resistant cells yielded 156.0±3.6 (n=3) hematopoietic-like colonies per 10^4 re-plated cells suggesting that the efficiency of reprogramming was at least 1.5% ($156/10^4$). This calculation assumes that each colony originates from a single reprogrammed cell. The efficiency is likely much higher in cells expressing the appropriate stoichiometric quantities of each factor.

Identification of viral integration on a single-cell and single-colony level

To identify the presence of viral integration on a single-cell level, we sorted human $CD45^+$ cells from the marrow of rEC-hMPP engrafted mice into a 96-well plate 1 cell per well into a lysis buffer for the Phi29 (multiple displacement amplification – MDA) based whole-genome amplification (WGA). To do single-cell WGA, we used a commercially available kit REPLI-g (Qiagen, Cat.No. 150343). Each WGA reaction product was followed by a set of PCR reaction with primers specific to the CMV promoter and a transgene (*FOSB, GFI1, RUNX1, SPI1*). All PCR reactions were conducted separately. We used empty wells (no cells sorted) as controls for non-specific amplification. WGA products of the control wells were used for PCR reactions with primers specific to the CMV promoter and a transgene.

To identify the presence of viral integration on a single-cell level, we captured expanding colonies from the plates for CFC assay. Fourteen days after the start of CFC assay 3 distinct cell aggregations/colonies were detected and analyzed (three upper images). Four PCR reactions were performed for each amplified colony using their genomic DNA as template. Cells from the colonies were re-suspended and washed twice in excessive amounts of PBS (10ml) and transferred into the lysis buffer for the WGA. All following procedures were the same as those described for the single-cell viral integration identification.

CMV primer: 5'-cgcaaatgggcggtaggcgtg-3'

FOSB primer: 5'-gctctgctttttcttcctccaact-3'

GFI1 primer: 5'-ccagggccccacacggtcggtagc-3'

RUNX1 primer: 5'ttgcggtgggtttgtgaagac-3'

SPI1 primer: 5'cggatcttcttcttgctgcctgtc-3'

Clonal reprogramming of HUVECs to rEC-hMPPs

HUVECs were isolated from umbilical cord and grown in EC-growth medium. After 2 to 3 passages, $CD144^{+}CD31^{+}CD62E(E\text{-selectin})^{+}CD45^{-}$ HUVECs were FACS sorted into 96-well plates at 1, 2, 5 and 10 cells per well densities for clonal expansion. We used CD62E (E-selectin) surface marker to sort mature activated ECs. Passaging of HUVECs results in upregulation of E-selectin in 40 to 60% of the HUVECs. Expanding clonal populations of selected cells were subsequently transduced with the FGRS TFs followed by replating onto the E4EC monolayers to reprogram them into rEC-hMPPs. Hematopoietic activity of clonally derived $CD45^{+}CD34^{+}$rEC-hMPPs was assessed using standard methylcellulose-CFC assay.

RNA-Seq processing and analysis

Total RNA was prepared using the Applied Biosystems Arcturus PicoPure RNA isolation kit. The quality of the extracted RNA was checked on an Agilent Technologies 2100 Bioanalyzer. The extracted RNA was used for sequencing using Illumina HiSeq2000. The sequencing output was checked for quality using Illumina pipeline. PE 51×2 and SE 51 reads were mapped to the human genome (hg18) using TopHat (http://tophat.cbcb.umd.edu/) default parameters. RefSeq transcript levels (FPKMs) were then quantified using CuffLinks (http://cufflinks.cbcb.umd.edu/) with upper-quartile normalization and sequence-specific bias correction. For heatmap visualization we determined the maximum FPKM of each transcript across the samples shown. FPKMs were then divided by this number to produce scaled expression values. Heatmaps of gene expression and gene expression clustering were built using GENE-E matrix visualization and analysis platform (http://www.broadinstitute.org/cancer/software/GENE-E/). Clustering of gene expression in the heat maps was conducted using one minus Pearson correlation as dissimilarity measure between transcription profiles. GEO accession number: GSE57662. The GSE57662 study can be reviewed at: http://www.ncbi.nlm.nih.gov/geo/query/acc.cgi?acc=GSE57662.

Comparative Genomic Hybridization (CGH)

Genomic DNA was extracted from HUVECs, FACS sorted $CD45^+$ rEC-hMPPs, and $CD45^+CD34^+$ rEC-hMPPs sorted from the BM of the NSG mice. Before DNA extraction, $CD45^+CD34^+$ rEC-hMPPs sorted from the BM were expanded for 72 hours *in vitro*. As a positive control of chromosomal rearrangements we used a CGH array of a leukemic cell line with a duplication of the chromosome 7 and a deletion of the chromosome 10. Extracted DNA was digested, labeled by random priming and hybridized to the Agilent 1M CGH arrays. The arrays were scanned in an Agilent DNA microarray scanner and obtained data was visualized using Feature Extraction software (version 10.7; Agilent).

Differentiation and reprogramming of human embryonic stem cells (hES)

We used a transgenic hES reporter line that specifically identifies differentiated EC derivatives via a fluorescent reporter driven by a fragment of the human VE-cadherin promoter[1,35]. To augment endothelial commitment, hES differentiation was initiated in co-culture with E4EC vascular niche cells, described above. One day before plating hES to begin differentiation, MEF conditioned medium was replaced with hES culture medium without FGF-2 and supplemented with 2 ng/ml BMP4. The next day, hES cells were plated directly onto E4EC monolayers in hES culture medium (without FGF-2, plus 2 ng/ml BMP4) and left undisturbed for 48 hours. This point of culture was considered as differentiation day zero. Cells were sequentially stimulated with recombinant cytokines in the following order: day 0 to 7 -supplemented with 10 ng/ml BMP4; day 2 to 14 - supplemented with 10 ng/ml VEGF-A; day 2 to 14 -supplemented with 5 ng/ml FGF-2; day 7 to 14 - supplemented with 10 μM SB-431542. At day 14 of culture, FACS sorting was used to purify the fraction of hES-derived ECs co-expressing the vascular specific CD144 (VE-cadherin) reporter and CD31. These cells were transduced with the FGRS cocktail and 2–3 days later plated on a layer of serum-free E4EC monolayers. The extent of reprogramming was assessed by flow cytometry.

Phagocytosis assay

The rEC-hMPPs generated from 3 to 4 weeks, were cultured in the presence of M-CSF (10ng/ml), SCF (10ng/ml), Flt-3 (10ng/ml), TPO (10ng/ml), and 10% FBS for additional two weeks with E4EC vascular niche layer. We observed an increase in size and granularity of the cultured cells (data not shown). The culture was washed with PBS twice to remove non-adherent cells. Growth media mixed with green fluorescent beads (GFB) at a low concentration of 1 μl/ml was applied to the attached cells for one hour at 37°C.After the incubation, the cells were washed twice with PBS and live cells were stained with the monocytic CD14 antibody. Cells were fixed and stained with DAPI for nuclear visualization. We visualized GFB inside $CD14^+$ cells, but not in CD144 $(VE\text{-cadherin})^+$ endothelial cells (Extended Data Figure 2G).

Purification of human cord blood stem and progenitors cells (HSPCs)

Human umbilical cord blood was obtained under the IRB protocol Stage “Specific Differentiation of Hematopoietic Stem Cells into Functional Hemangiogenic Tissue” (Weill Cornell Medical College IRB # 09060010445). Cord blood mononuclear cells were purified

by density gradient using Ficoll-Paque (GE) and enriched for $CD34^+$HSPC using magnetic separation using anti-CD34 microbeads (Miltenyi) or FACS sorting. Further purification was achieved by negative selection of Lin^+ cells using Human Progenitor Cell Enrichment Kit (StemCell Technologies) or FACS sorting. RNA from FACS sorted $Lin^-CD34^+CD45^+$ cells was isolated by using Arcturus PicoPure RNA isolation kit (Applied Biosystems; This kit was used for all RNA extraction procedures).

Lentiviral vectors

Candidate transcription factors (TFs) were subcloned into either pLVX-IRES-ZsGreen1 lentivector (Clontech), pLOC lentivector (OpenBiosystems), or LV105 lentivector (Genecopoeia). For inducible expression of mouse or human FGRS factors we used Tet-On 3G inducible lentiviral vectors (Clontech). Lentiviral particles were packaged as previously described[7]. In short, human embryonic kidney 293FT (HEK293FT) cells were co-transfected with a lentivector and two helper plasmids psPAX2, and pMD2.G (Trono Lab through Addgene) in the equal molar ratio. Supernatant was collected 48–52 hours post-transfection, filtered and concentrated using Lenti-X concentrator (Clontech). Viral titers were determined in limiting dilution experiments using HUVECs as target cells. We used either the number of GFP^+ cells, or the number of formed colonies in the presence of selection antibiotics (puromycin) as a read-out for the number of infectious viral particles per volume. We used an average MOI of 5 to 10 for infection of ECs.

Flow Cytometry

Flow cytometry analysis was performed on a Becton Dickenson LSRII SORP, and fluorescence activated cell sorting (FACS) was performed on an Aria II SORP. Antibodies used were raised against human CD45, CD34, CD14, CD31, CD43, CD90, CD41a, CD33, CD19, CD3, CD4, CD8, CD235, CD45RA, CD83, CD11b, CD38, LIN cocktail, CD117, CD133, CD144 (BD Pharmingen, eBioscience) or mouse CD45 (eBioscience.) Voltage adjustments and compensation was performed with CompBeads (BD Pharmingen), and gating was performed on fluorophore minus one (FMO) controls and unstained controls.

The list of antibodies used in our experiments:

Anti-human antibodies obtained from EBioscience:

CD45 Cat# 47–0459-42; clone HI30, CD34 Cat# 25–0349-42; clone 4H11, CD33 Cat# 48–0337-42; clone p67.6, CD19 Cat# 12–0199-41; clone HIB19, CD3 Cat# 93-0037–42; clone OKT3, CD4 Cat# 17–0048-41; clone OKT4, CD8 Cat# 8048-0087-025; clone SK1, CD43 Cat# 17–0439-73; clone eBio84-3C1, CD83 Cat# 25–0839-41; clone HB15e, CD11b Cat# 12–0118-41; clone ICRF44, LIN Cat# 22–7778-72, CD31 Cat# 11–0319-42; clone WM59, CD31 Cat# 48–0319-42; clone WM59

Anti-human antibodies obtained from BD Pharmigen:

CD90 Cat# 561971; clone 5E10, CD3 Cat# 557851; clone SK7, CD14 Cat# 557742, CD14 Cat# 555399, CD235A Cat# 340947, CD45RA Cat# 347723, CD41a Cat# 555466, CD38

Cat# 646851, CD117 Cat# 333944, CD33 Cat# 333946, CD144 Cat# 560410; clone 55-7H1, FLK1(VEGF-R2) Cat# 560871; clone 89106

Anti-human antibodies obtained from BioLegend:

Lin Cat# 348805

Anti-mouse antibodies obtained from Ebioscience:

CD45 Cat# 25–0451-82; clone 30-f11

Statistics and Animals

All statistics is presented as average ±standard deviation. To identify statistical significance all groups of data were compared using paired student t-test.

Experiments were repeated for at least three times. Number of repeats is demonstrated in all figure legends.

Animal experiments contain at least three animals per group. The number of animals is described in all figure legends and the text of the paper.

We included all tested animals for quantification. Representative images and flow cytometry plots are shown in the figures.

Age and sex-matched animals were allocated in all corresponding experimental groups. All NSG animals for transplantation experiments were female. All ages are specified in the text. Animals were chosen according to their age and their sex (females only). A description of every experiment states the age of the animals used in the experiment.

Transplanted animals were not individually labeled. Hence, subgroups of transplanted animals for organ engraftment were chosen blindly, without prior knowledge of the level of engraftment.

Animal experiments were performed under the guidelines set by the Institutional Animal Care and Use Committee (IACUC).

Extended Data

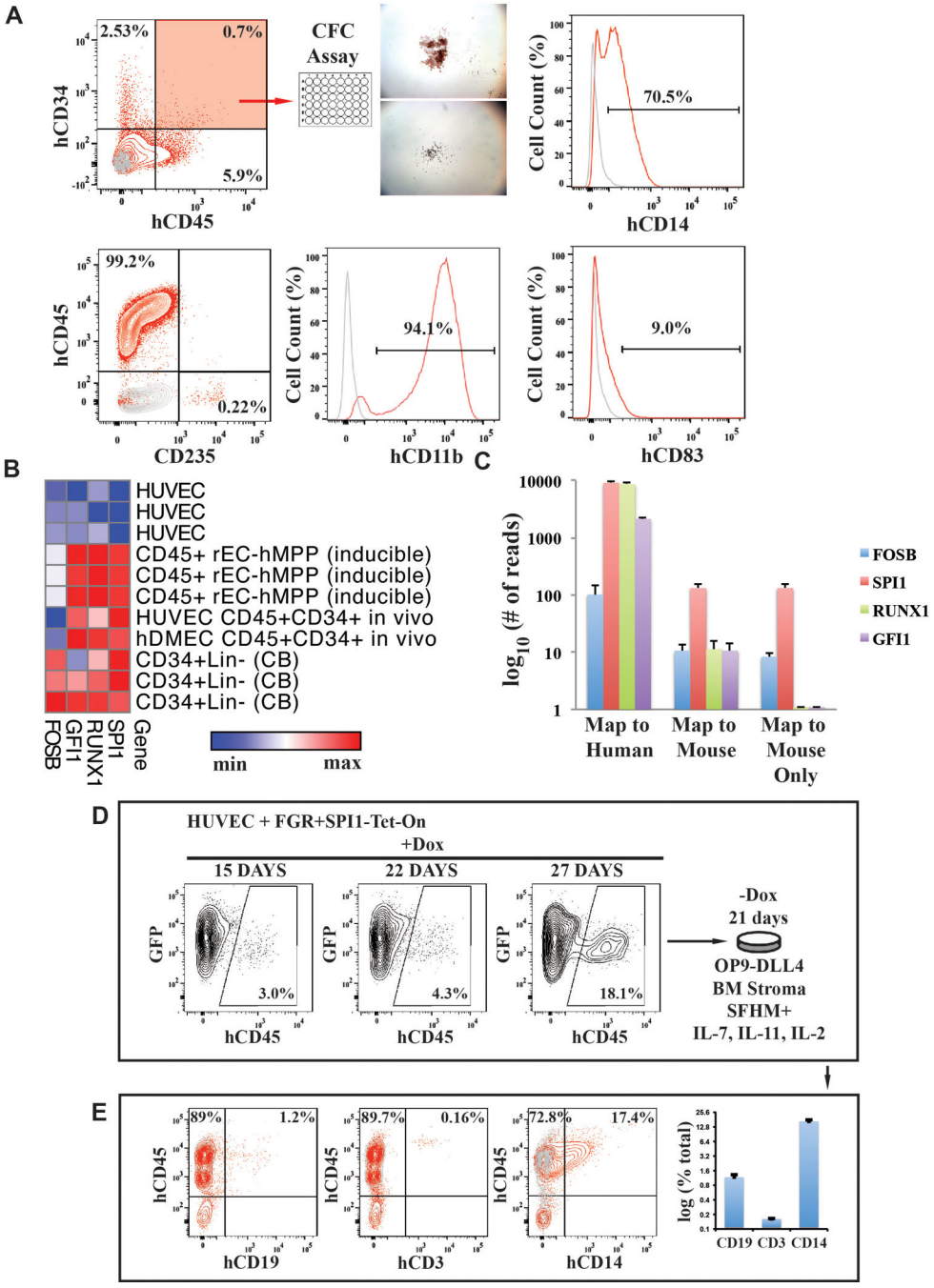

Extended Data Figure 1. Screening strategy for identification of minimal set of transcriptions factors (TFs) for reprogramming ECs into hematopoietic cells

A. Candidate genes tested for reprogramming of HUVECs into hematopoietic colonies. To identify TFs that drive EHT transition, we performed RNA-seq of HUVECs and Lin-CD34^{+} umbilical cord HSPCs to select TFs differentially expressed by HSPCs, but not by HUVECs. We then screened various combinations of differentially expressed TFs to identify a minimal set capable of reprogramming ECs to hematopoietic cells. Levels of

expression [$\log_2$(RNA-seq value)] in HUVECs and freshly purified $CD34^+Lin^-$ cord blood cells.

B. One-by-one elimination of TFs experiment revealed a minimal set of TFs; *FOSB, GFI1, RUNX1*, and *SPI1*, (FGRS) capable of generating hematopoietic colonies in the HUVEC culture. A pulled set of 26 TFs minus one TF was evaluated for the ability to evoke formation of hematopoietic clusters (day 21 to 25; n=3). Asterisks show statistically significant ($p<0.05$) reduction of the number of hematopoietic clusters in the transduced HUVECs compared to the full set of TFs. Control represents non-transduced HUVECs. Transduced cells were cultured on a layer of serum-free E4EC monolayers.

C. One-by-one elimination of the FGRS factors shows that all four FGRS-TFs are necessary and sufficient for generation of hematopoietic colonies (day21 to 25; n=3).

"**All**" in **B** and **C:** all TFs are present. "**Control**" in **B** and **C**: all TFs are absent.

D. Schema for reprogramming of ECs into human multipotent progenitor cells (rEC-hMPPs). Clonal or bulk populations of HUVECs or hDMECs were transduced with the FGRS and after 3 days were replated on subconfluent monolayers of E4EC ECs. The emerging colonies of hematopoietic cells were subjected to 1) multi-variate immunophenotypic analyses, 2) clonal and oligo-clonal CFC assay, and 3) molecular profiling (RNA-seq). Tissues of the engrafted mice were processed for histological examination to rule out any malignant transformation.

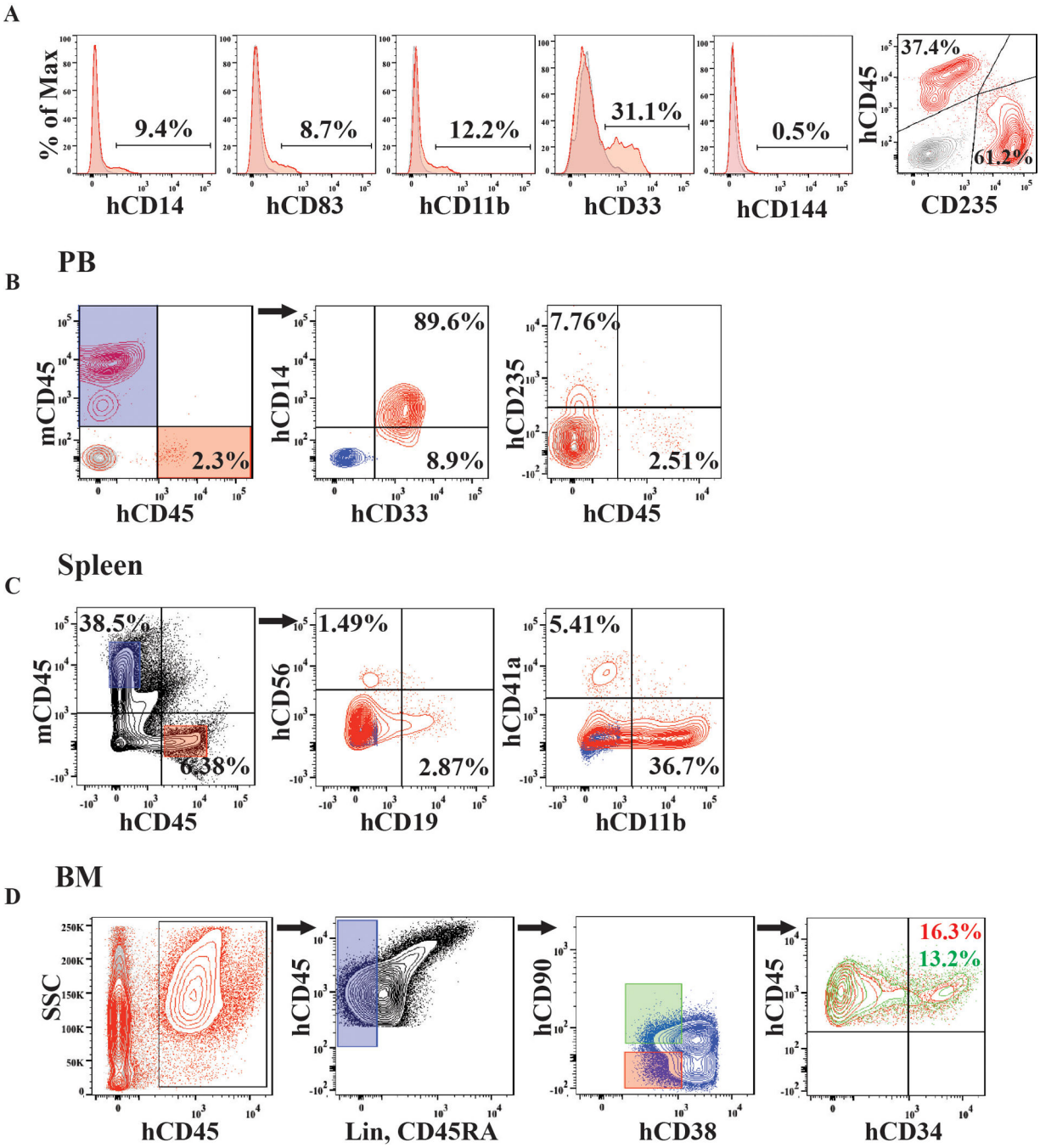

Extended Data Figure 2. FGRS-transduction and vascular-induction reprogram HUVECs, but not hES-ECs, to proliferating functional rEC-MPPs

A. Multi-colony niche-like structure that physically separates developing hematopoietic colonies from surrounding E4EC vascular niche. The emerging multi-colony sinusoidal-like structures create a unique cellular interface between E4EC monolayers and transduced ECs giving rise to hematopoietic clusters (n=4, scale bar is 1000 μm.)

B. Expansion potential of reprogrammed CD45^{+}hematopoietic cells. CD45^{+} (12×103) and CD45- (60 ×10^{3}) cells were sorted into separate wells and expanded for two days. We

observed 5-fold expansion of $CD45^+$ cells ($56.6 \times 10^3 \pm 7.9 \times 10^3$; n=3) and dramatic reduction of $CD45^-$ cells number ($4.6 \times 10^3 \pm 1.0 \times 10^3$; n=3).

C. Clonal expansion of $CD45^+$ cells. $CD45^+$cells were FACS sorted into 96-well plates at the density of 1 and 2 cells/well. After seven days of culture, we observed $CD45^+$ cell expansion in 6.3±2.1 wells (93.1±14.5 cells/well) of 1-cell sort and 29.0±4.3 wells (112.1±21.2 cells/well) of the 2-cell sort (n=3). The difference between cell number in 1 and 2-cell sort was statistically not significant (p=0.78) suggesting that the difference in the number of wells with detected cell expansion was rather due to survival of sorted cells than a reflection of the number of cells sorted into a well.

D. FGRS-induced generation of hematopoietic cells by hES-derived endothelium (hES-EC). Representative experiment demonstrating that transduced hES-EC (Right 4 panels) generated significantly higher number of $CD45^+$CD144- cells compared to control non-transduced hES-EC (left 3 panels).

E. Lineage-specific surface marker analysis of the GFP^+CD45+ population of rEC-hMPPs. GFP^+CD45^+population showed that some of these cells expressed lineage specific surface markers such as $CD43^+$ (8.96%±2.3; n=3), $CD90^+$ (Thy-1^+) (6.15%±1.13; n=3) and $CD14^+$ (40.0%±4.95; n=3) (representative flow cytometry measurements; left four panels, statistics for all experiments is in the right-hand bar-graph, n=3).

F. Immunophenotypic analysis of CFU colonies grown in the CFC assay performed in Figure 2C,D.

G. Macrophages differentiated from rEC-hMPPs are functional capable of phagocytosis. The images (upper row and lower left) show groups of firmly plastic-adherent $CD14^+$ cells (red staining) with clearly visible phagocytosed green fluorescent beads (GFB; green). Endothelial $CD144^+$(VE-cadherin) cells (white staining) were not co-localized with beads. Majority (85.1%±15.1) of GFBs was localized inside $CD14^+$ cells (lower left graph **1**). A smaller population of GFBs was distributed outside $CD14^+$ and CD144(VE-cadherin)$^+$ cells (14.8±7.43%; lower left graph **2**). The percentage GFBs co-localized with endothelial cells was negligible (4.8±0.83%; lower left graph **3**), n=9.

Scale bars are 25 μm.

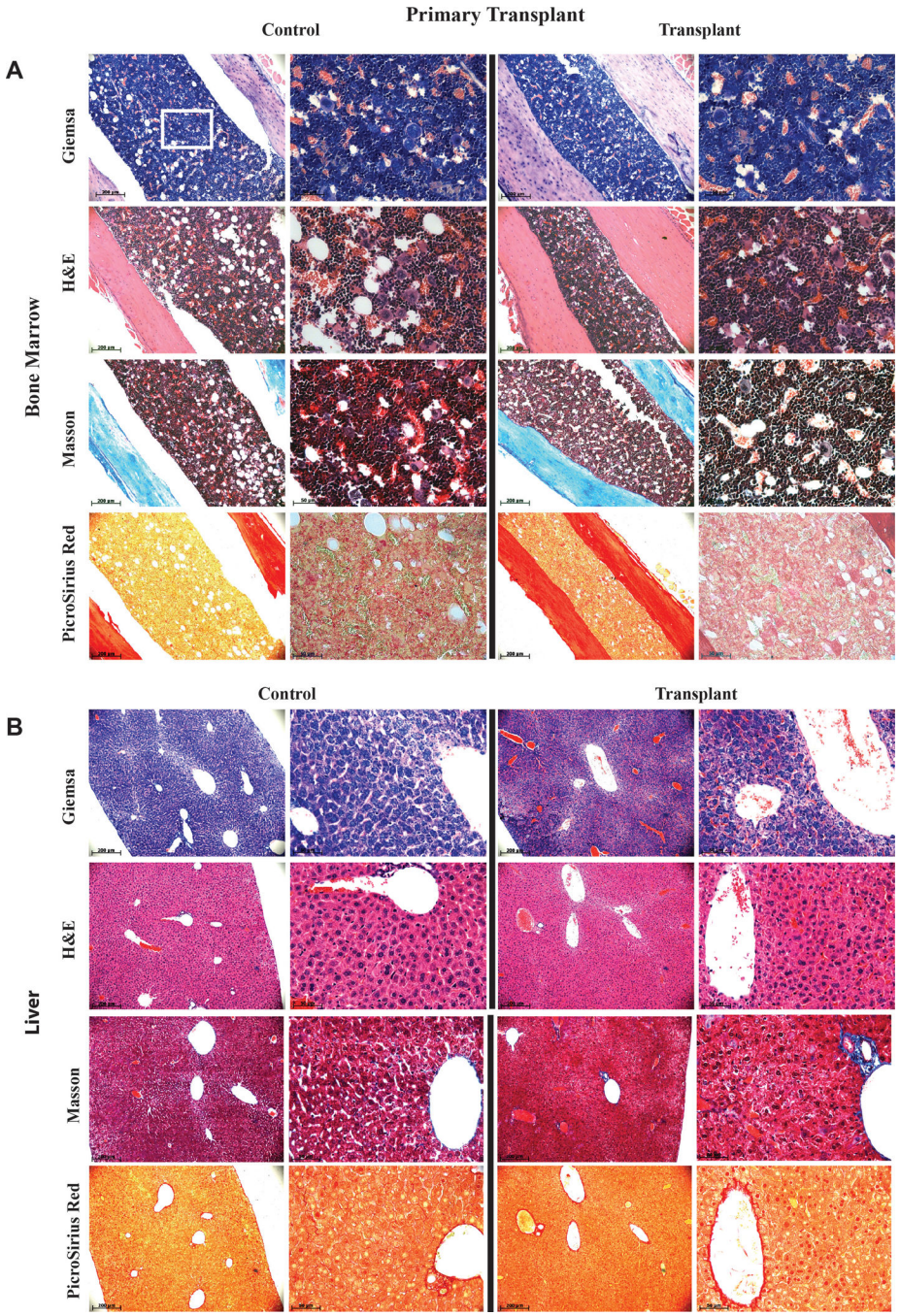

Extended Data Figure 3. Naïve HUVECs are devoid of hemogenic potential capable of spontaneous differentiation into MPPs

We performed two sets of experiments to exclude the possibility that rEC-hMPPs were derived from spontaneously differentiating HUVECs with hemogenic or hemangioblastic potential[25,34].

A to B: In optimal pro-hematopoietic cultures, naïve non-transduced ECs fail to spontaneously differentiate into rEC-MPPs.

A. We grew non-FGRS-transduced HUVECs in the serum-free media used for reprogramming. Neither serum withdrawal, nor addition of hematopoietic cytokines induced formation of $CD45^{+}CD34^{+}$ cells and HUVECs sustained their vascular identity. Indeed, serum withdrawal increases number of $CD34^{+}$ HUVECs; SF-serum free, CK-cytokines cocktail (see methods), SB - TGFβ inhibitor SB431542.

B. Serum withdrawal suppresses HUVEC proliferation. Inhibition of TGFβ signaling (SB) combined with cytokine cocktail (see methods) restores proliferative potential of HUVECs in serum free media. Difference between proliferation of HUVECs in serum free media and all other conditions is statistically significant (asterisk; $p<0.005$). Statistical significance between pairs of different conditions is shown with blue arrows and p-values, where $p<0.005$ is statistically significant. Therefore, human rEC-hMPPs originate from reprogrammed ECs, but not cytokine-mediated outgrowth of contaminating pre-existing hemogenic ECs.

C to E: Clonal reprogramming of non-hemogenic HUVECs into rEC-hMPPs using FGRS-transduction and vascular-induction.

We performed EC clonal reprogramming experiments to exclude the possibility that rEC-hMPPs were derived from spontaneously differentiating HUVECs with pre-existing hemogenic or hemangioblastic potential[25,34].

C. Since E-selectin is only expressed in ECs, we generated clonal cultures of $CD45^{-}CD144^{+}CD31^{+}CD62E(E\text{-selectin})^{+}$ ECs[32,33]. To this end, CD144+$CD31^{+}CD62E^{+}CD45^{-}$HUVECs were sorted into 96-well plates at 1, 2, 5 and 10 cells per well densities for clonal expansion. Proliferating clones were transduced with FGRS and induced with serum-free E4ECs. **D**. These clonal cultures yielded rEC-hMPPs comparable to bulk HUVEC cultures. The numbers of hematopoietic-like colonies emerging from 1-cell, 2-cell, 5-cell, and 10-cell clones are not statistically different ($p>0.05$). **E**. An example of a hematopoietic-like colony derived from a 1-cell clone #2. Therefore, it is unlikely that rEC-hMPPs are derived through spontaneous differentiation of pre-existing ECs with hemogenic or hemangioblastic potential.

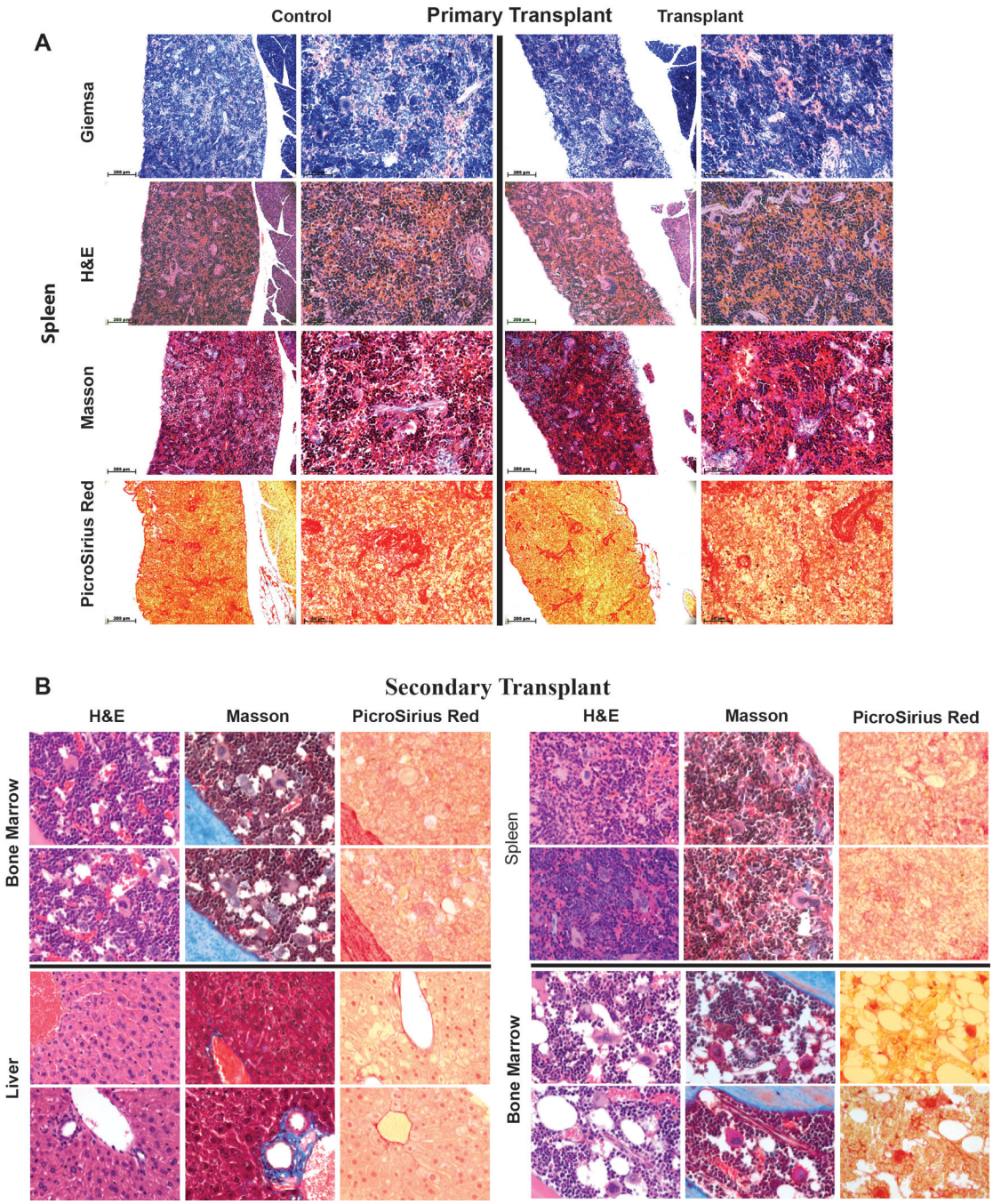

Extended Data Figure 4. Clonal reprogramming of non-hemogenic HUVECs into immunophenotypic and functional rEC-hMPPs using FGRS-transduction and vascular-induction

A,B,C: CFC assay of clonally reprogrammed rEC-hMPPs. $CD45^{+}CD34^{+}$rEC-hMPPs were sorted out (red gate in FACS plots; upper left) and plated for CFC assay. Typical hematopoietic colonies arose in the assay (middle column microphotographs; x4 magnification). FACS plots on the right show immunophenotypic analysis of the cells that arose in the CFC assay, demonstrating differentiation into human $CD45^{-}CD235^{+}$erythroid $CD11b^{+}$macrophage $CD14^{+}$monocytic, $CD41a^{+}$megakaryocytic and $CD83^{+}$dendritic

progenies. The graph in the left lower corner shows quantification of the CFC assay (n=3). Identical panels are shown for two 2-cell clones and one 5-cell clone. A total of 3 independent clones are shown. Thus, given the high efficiency of clonal reprogramming of mature authentic ECs into rEC-hMPPs, it is unlikely that rEC-hMPPs are spontaneously derived from a very rare population of a pre-existing hemogenic or hemangioblastic HUVECs.

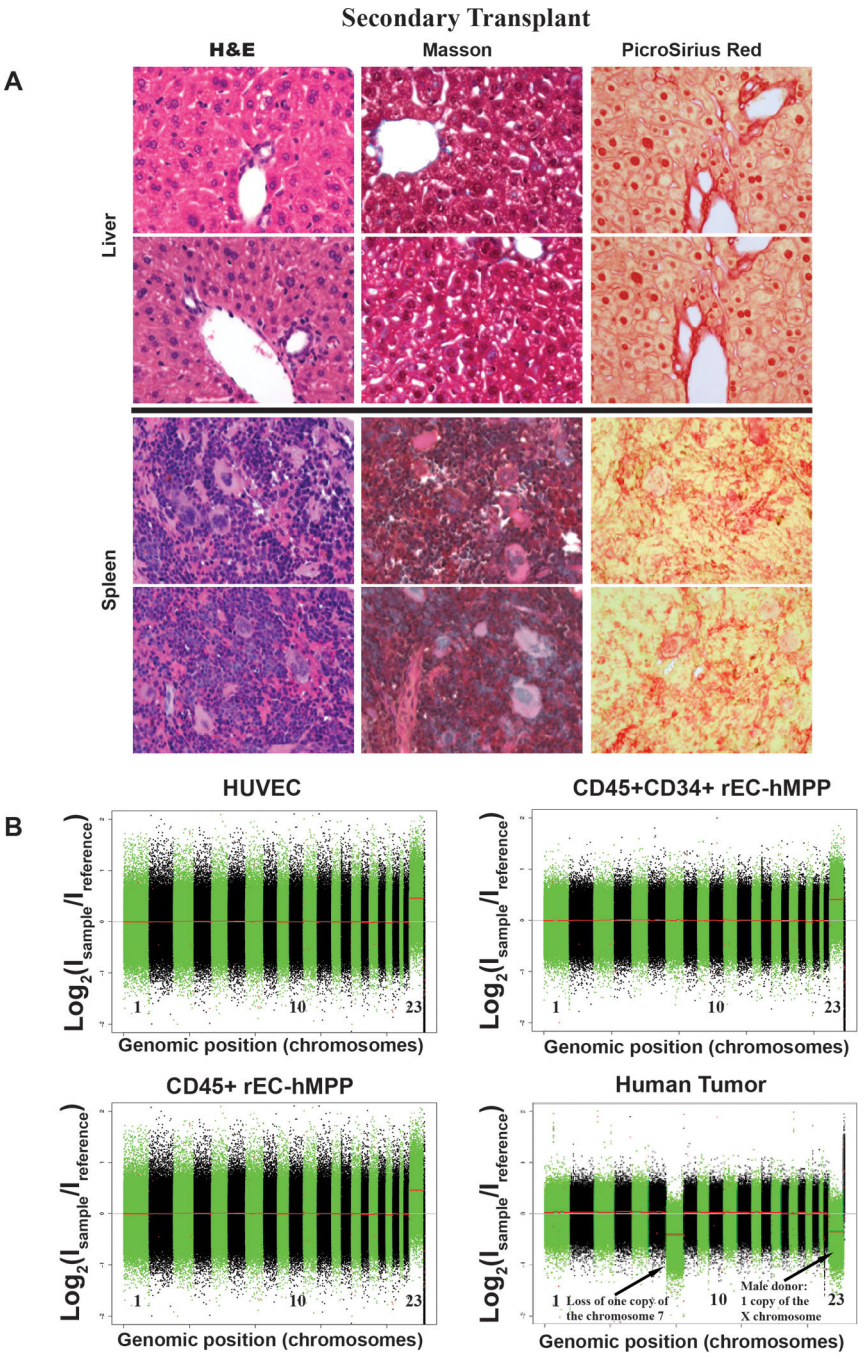

Extended Data Figure 5. Single cell analysis of lentiviral integration into engrafted rEC-MPPs

$CD45^+$ cells were sorted into a 96-well plate (1 cell/well), lysed in corresponding well for whole genome amplification (WGA) using Phi29 enzyme (see methods). Amplified DNA is shown for all 21 cells in the top two gels. Amplified DNA was used as a template for PCR reactions with a forward primer specific for the CMV promoter and reverse primer specific for the coding sequence of a reprogramming factor. T-test PCR with a lentiviral vector. EW – empty well – no template DNA. Red asterisks show failed PCR amplification of viral integration. PCR products are visible as low molecular weight bands labeled as 1 – *FOSB*, 2 – *GFI1*, 3 – *RUNX1*, 4 – *SPI1*.

A

ORF	HUVEC	CD34+Lin- (CB)
ZFP36	4.81	12.40
FOS	3.82	12.36
JUNB	6.26	12.17
GMFG	5.33	10.30
KLF2	7.70	10.28
FOSB	1.51	10.28
NFE2	0.00	9.45
KLF1	0.00	9.29
LYL1	8.55	9.03
LMO2	7.24	8.87
TAL1	6.20	8.31
GATA1	0.00	8.18
SPI1	0.00	8.04
IKZF1	0.00	7.83
GFI1B	0.00	7.70
VAV1	0.00	7.67
MEIS1	3.23	6.75
MYB	0.23	6.47
MLLT3	4.21	6.40
RUNX1	0.21	6.23
GFI1	0.00	5.54
HLF	0.00	4.67
BEX1	2.52	4.47
PBX1	4.24	4.88
BEX2	0.03	3.95

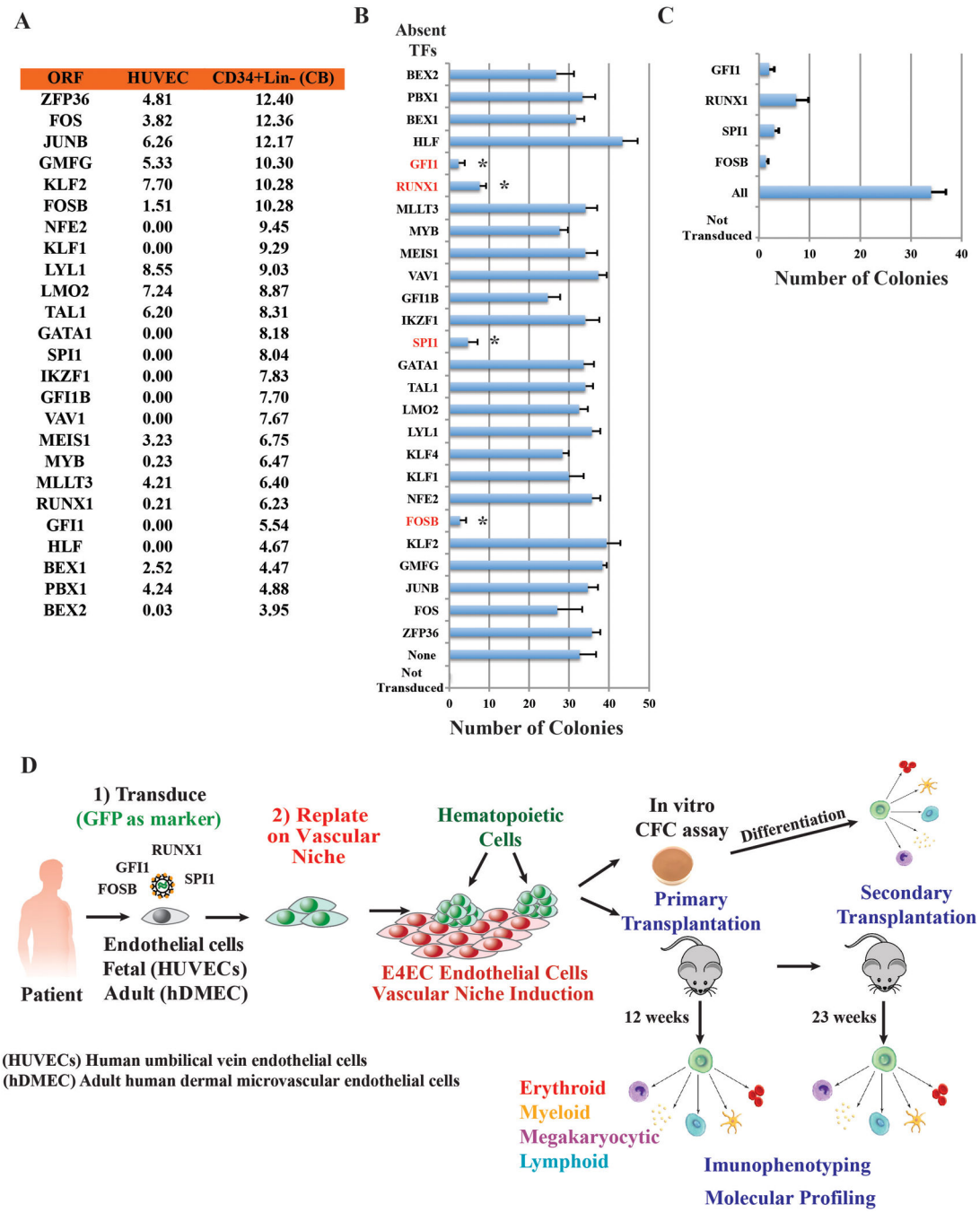

Extended Data Figure 6. Conditional expression of FGRS is sufficient for optimal generation of rEC-hMPPs with multilineage potential, including T-Cell lymphoid cells

A to C: Conditional expression of mouse inducible FGRS factors activates endogenous human FGRS in HUVECs sustaining functional hematopoietic cell fate of rEC-hMPPs.

A. To test whether FGRS-induced reprogramming triggered expression of endogenous FGRS genes[24], HUVECs were transduced with lentivirus expressing FGRS-Tet-On and a trans-activator, and grown on E4EC-vascular niche for 18–22 days (n=4) in the presence of doxycycline. Doxycycline was removed from the culture medium after 18–22 days to shut

off the expression of mouse FGRS and cells were cultured for additional 7–10 days. Human $CD45^+CD34^+$ cells were FACS isolated for CFC assay and whole-transcriptome deep sequencing (RNA-seq). CFC assay revealed emergence of hematopoietic colonies with cells expressing human CD235, CD11b, CD83, and CD14. **B**. Comparison of transcriptional profiles of the human FGRS expression in human HUVECs, $hCD45^+$ rEC-hMPPs programmed using inducible mouse FGRS, $CD45^+CD34^+$ rEC-hMPPs, 22 weeks post-transplantation, hDMEC-derived $CD45^+CD34^+rEC^-$ hMPPs after 15 weeks post-secondary engraftment and naïve $CD34^+Lin^+$ cells purified from cord blood.

C. Analysis of whole-transcriptome RNA-Seq of rEC-hMPPs derived using inducible mouse FGRS (n=3). All RNA-Seq reads were aligned against human and mouse FGRS sequences. RNA-Seq reads that align to human FGRS sequences – “Map to Human”, RNA-Seq reads that align to mouse FGRS sequences – “Map to Mouse”, and RNA-Seq reads that align to mouse FGRS sequences without a possibility to align to human sequences – “Map to mouse Only”.

D to E: Optimizing differentiation of rEC-hMPPs into lymphoid progeny

D. The number of T-lymphoid progeny of engrafted rEC-hMPP was negligibly small, raising the possibility that constitutive SPI1 expression prevents rEC-hMPP from differentiating into T-cells[39,40]. To test this, HUVECs were transduced with lentiviral vectors expressing GFP and that constitutively express FGR-TFs with a Tet-inducible *SPI1* (FGR+*SPI1*-Tet-On construct) for 3 days followed by replating for E4EC-induction. After 27 days of FGR and doxycycline-induced *SPI1* expression on E4ECs, GFP^+CD45^+ hematopoietic-like colonies emerged. Then, doxycycline was withdrawn and the reprogrammed cells were cultured serum-free with Delta-like-4 expressing OP9-stroma (OP9-DLL4) supplemented with IL-7, IL-11, and IL-2. There is an increase of the number of GFP^+CD45^+ cells emerging during reprogramming of HUVECs by FGR+*SPI1*-Tet-On construct and E4EC-induction.

E. rEC-hMPPs differentiate into $CD3^+$, $CD19^+$ and $CD14^+$ hematopoietic cells in the absence of exogenous expression of *SPI1*. After 3 weeks, the numbers of the myeloid and lymphoid cells were quantified by flow cytometry. We were able to reliably detect a small fraction of $CD3^+$ cells (0.16±0.01%; n=3), a larger number of $CD19^+$ (1.17±0.13%; n=3) and $CD14^+$ (16.46±1.02%; n=3) cells. Thus, generation of lymphoid cells from rEC-hMPPs could be optimized by transient expression of TFs.

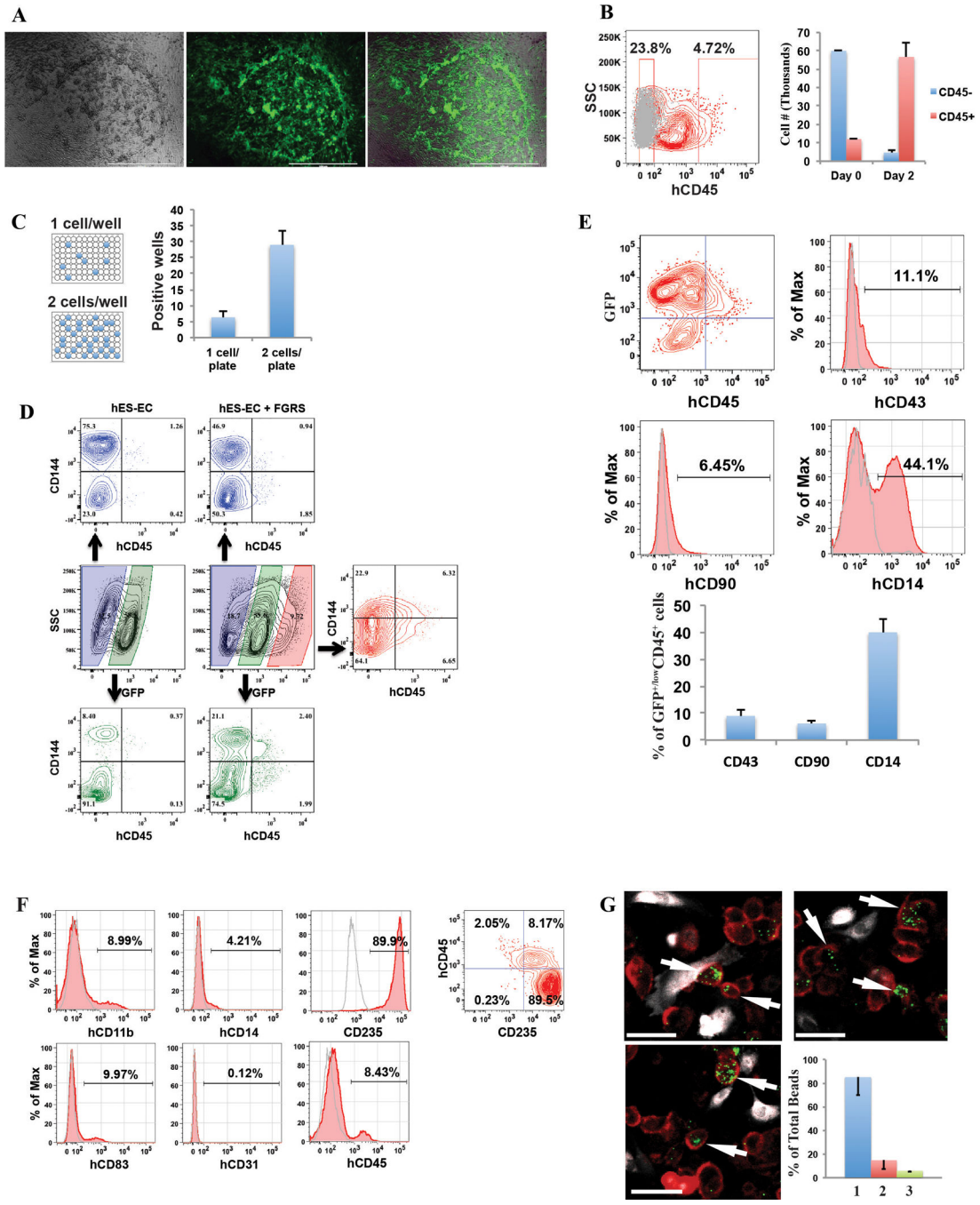

Extended Data Figure 7. Adult human hDMECs-derived rEC-hMPPs are capable of in vivo primary and secondary multilineage engraftment

A. Immunophenotypic analysis of cells grown in the CFC assay (from Figure 4B). These panels show quantification of surface marker expression in the cells isolated from the colonies in CFC assay (n=3). hDMECs differentiated into $hCD45^{-}CD235^{+}$ erythroid, $CD11b^{+}CD14^{+}$ monocyte/macrophage and $CD83^{+}$ dendritic cell progenies. Minimal CD144 (VE-cadherin) was detected.

B. Analysis of peripheral blood (PB) of mice at 4, 6, and 12 weeks post-primary transplantation (Figure 5A) revealed circulating $hCD45^+$ and their $hCD33^+$, $hCD14^+$myeloid and $hCD45^-hCD235^+$erythroid progenies (n=6). Mouse CD45 ($mCD45^+$) cells were excluded from analyses. Mouse cells – blue. Human cells – red.

C. Analysis of spleen of mice at 14 weeks post-primary transplantation (Figure 5A) revealed presence of $hCD45^+$ (Red gate) and their lymphoid ($hCD19^+$, $hCD56^+$) and myeloid ($hCD11b^+$, $hCD41a^+$) progenies (n=3). Mouse CD45 ($mCD45^+$ cells, blue populations).

D. Analysis of mice BM at 14 weeks post-primary transplantation (Figure 5A). $Lin^-CD45RA$ cells (blue gate) was analyzed for CD38 and CD90 expression (green and red gates) and subsequently examined for human CD45 and CD34 expression. This analysis revealed presence of $hCD34^+$cells with small populations of both $Lin^-CD45RA^-CD38^-CD90^+CD34^+$ and $Lin^-CD45RA^-CD38^-CD90^-CD34^+$ cells satisfying phenotypic definition of human HSCs and MPP, respectively (n=3).

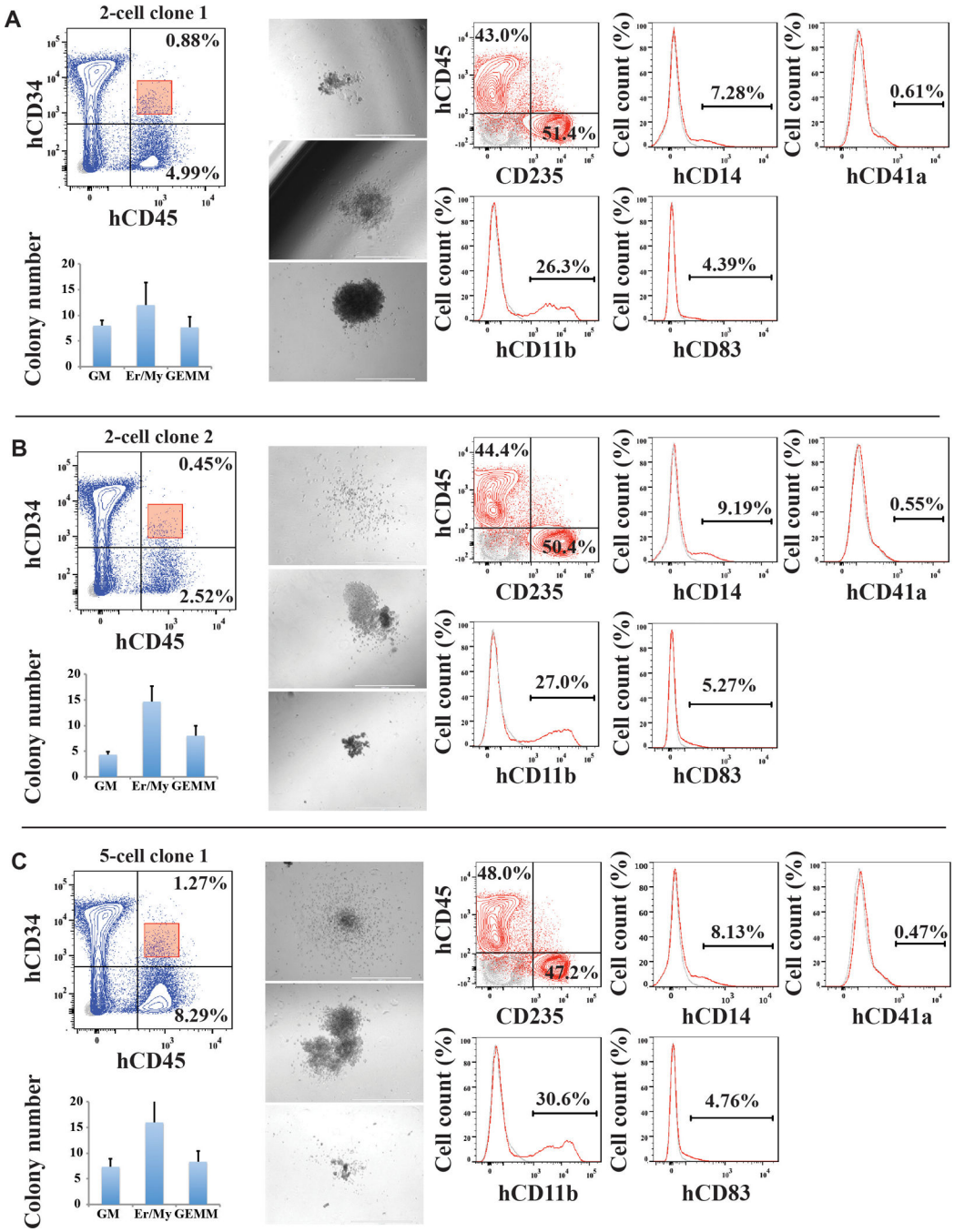

Extended Data Figure 8. Analysis of bone marrow (BM) and liver of primary transplanted mice for signs of malignant transformation

Analysis of BM (**A**) and liver (**B**) of mice 10 months after primary transplantation (from Figure 3B) of HUVEC derived rEC-hMPPs for signs of malignant transformation. The level of fibrosis was determined using Masson and PicroSirus staining. The architectonic geometry of the BM was determined by sequential multi-cross sectional Wright Giemsa and Hematoxylin-Eosin (H&E) staining and compared to age control non-transplanted NSG mice. We did not observe any evidence of fibrosis or alteration of the geometry of the bone

marrow or liver of the transplanted mice. Furthermore, no recipient mouse manifested any anatomical or symptomatic evidence of leukemias, lymphomas or myeloproliferative neoplasm (MPN): lymphadenopathy, organomegaly, illness or hemorrhage. Circulating $hCD45^+$ cells in PB displayed no evidence of lympho/myeloproliferation or dysplasia. Furthermore, microscopic architecture of BM and liver was normal and without fibrotic remodeling or aberrant deposition of collagen or desmin. All images were acquired using color CCD camera. The scale bar is 200μm for low-resolution images in the left columns and 50 μm for high-resolution images in the right columns. Upper left image (Giemsa Control) shows a white square in the center that corresponds to the portion of the image shown at high resolution on the right (the same Giemsa Control sample). This rule applies to all shown images.

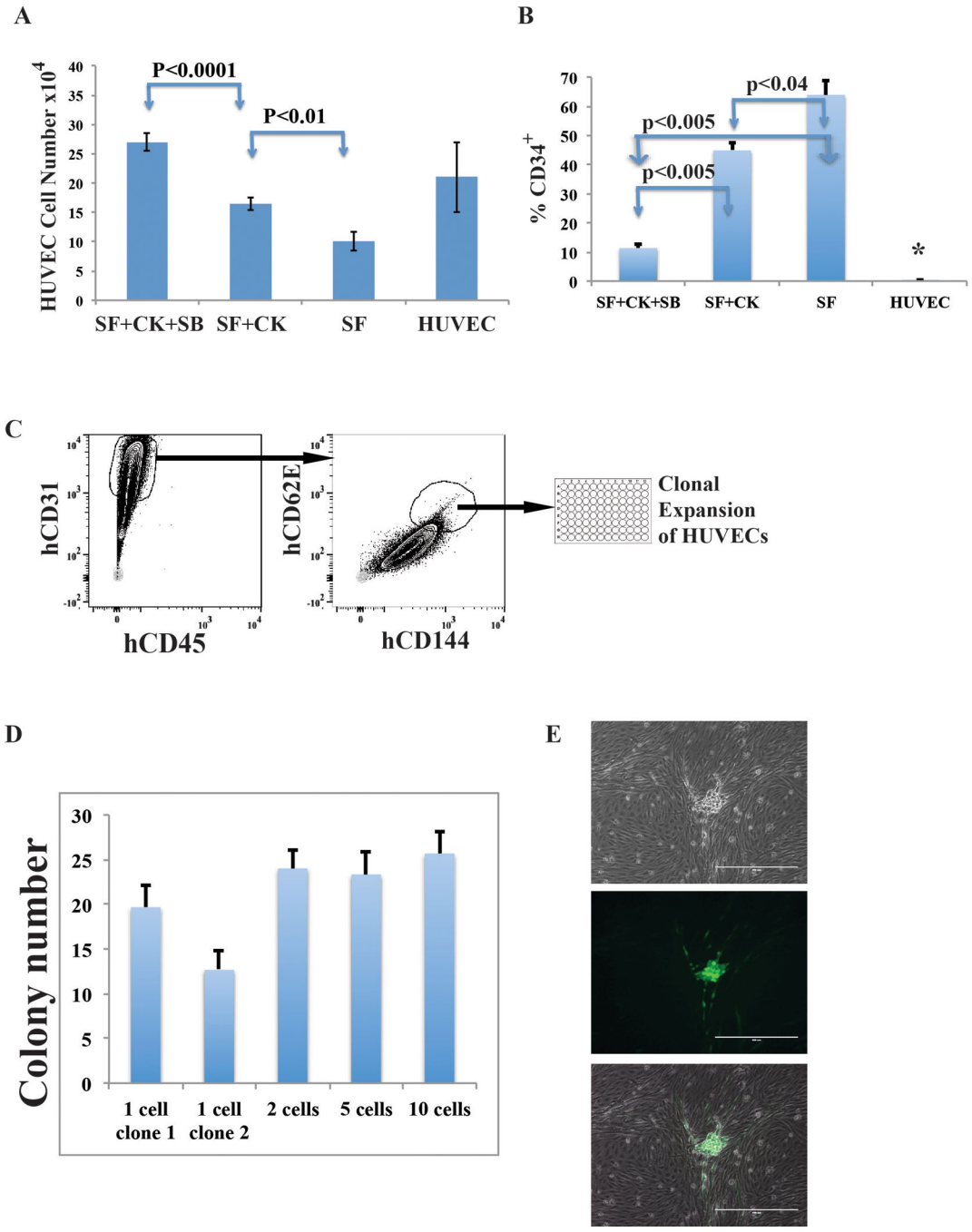

Extended Data Figure 9. Analysis of spleen of primary transplanted mice and BM, spleen and liver of secondary transplanted mice for signs of malignant transformation

Analysis of spleen of mice 10 months after primary transplantation (from Figure 3B) of HUVEC derived rEC-hMPPs as well as BM (n=2), spleen- and liver- (n=2, Also Extended Data Figure 10A) of mice that were engrafted with secondary transplanted hDMEC-derived rEC-hMPP cells 15 weeks post-transplantation (from Figure 5B) for signs of malignant transformation. The level of fibrosis was determined using Masson and PicroSirus stainings. The architectonic geometry of the BM was determined by sequential multi-cross sectional Wright Giemsa and Hematoxylin-Eosin (H&E) staining and compared to age control non-

transplanted NSG mice. We did not observe any evidence of fibrosis or alteration of the geometry of the bone marrow, spleen or liver of the transplanted mice. Furthermore, no recipient mouse manifested any anatomical or symptomatic evidence of leukemias, lymphomas or myeloproliferative neoplasm (MPN): lymphadenopathy, splenomegaly/organomegaly, illness or hemorrhage. Circulating $hCD45^+$ cells in PB displayed no evidence of lympho/myeloproliferation or dysplasia. Furthermore, microscopic architecture of BM, spleen and liver was normal and without fibrotic remodeling or aberrant deposition of collagen or desmin.

All images were acquired using color CCD camera. In primary transplants the scale bar is 200μm for low-resolution images in the left columns and 50 μm for high-resolution images in the right columns. Upper left image (Giemsa Control) shows a white square in the center that corresponds to the portion of the image shown at high resolution on the right (the same Giemsa Control sample). This rule applies to all shown images (Primary Transplant). All images in Secondary Transplant are acquired at 60x magnification. All images are acquired at 60x magnification. Top rows of images for each organ are secondary transplants; bottom rows of images for each organ are controls.

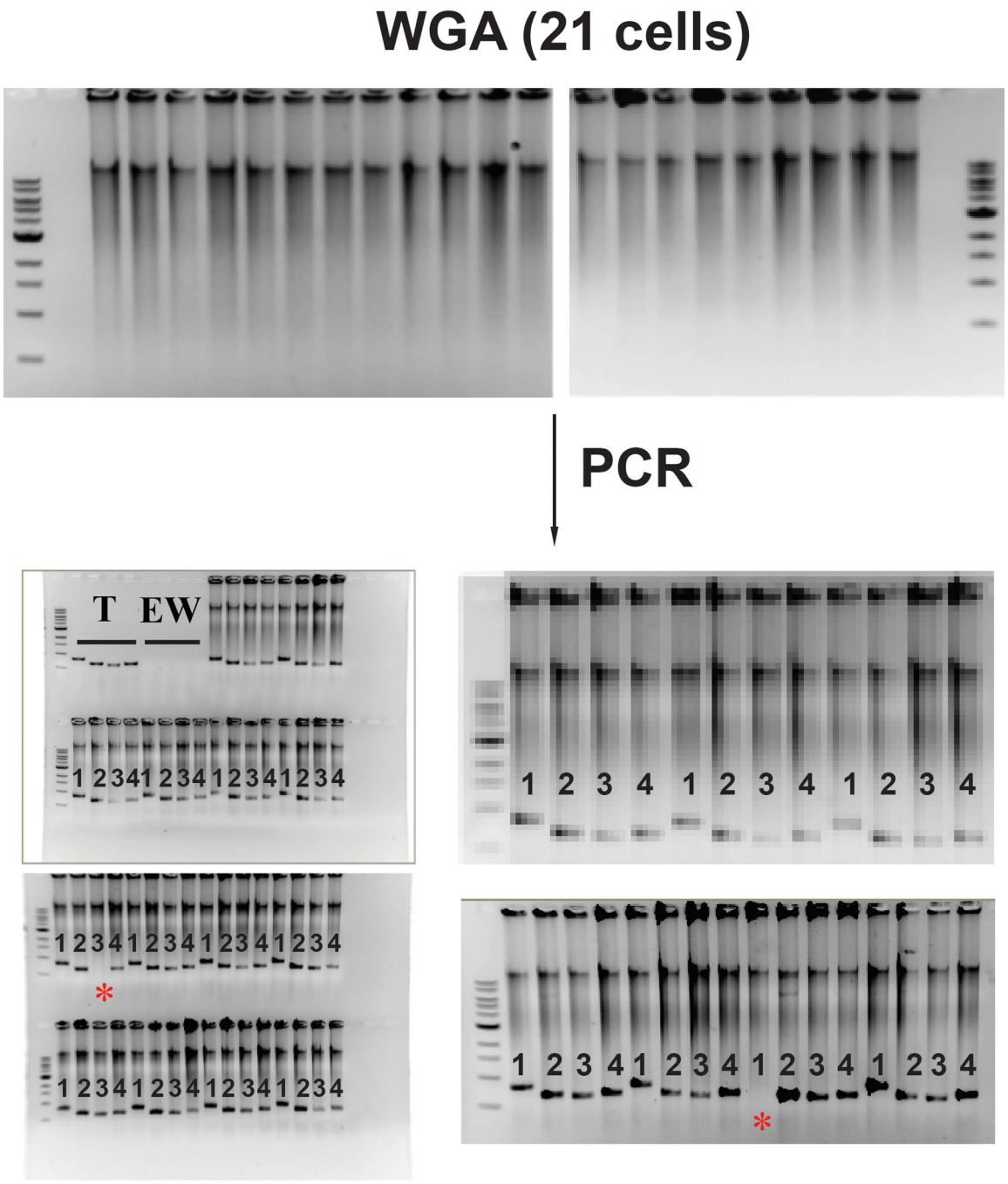

Extended Data Figure 10. Analysis of liver and spleen of secondary transplanted mice for signs of malignant transformation and analyses of rEC-MPPs for genetic stability

A. Analysis of liver and spleen of secondary transplanted mice for signs of malignant transformation. Repeat analysis of spleen and liver of mice that were engrafted with secondary transplanted hDMEC-derived rEC-hMPP cells 15 weeks post-transplantation for signs of malignant transformation (from Figure 5B). The level of fibrosis was determined by Masson and PicroSirus stainings. The architectonic geometry of the BM was determined by sequential multi-cross sectional Hematoxylin-Eosin (H&E) staining and compared to age

control non-transplanted NSG mice. We did not observe any evidence of fibrosis or alteration of the geometry of the spleen or liver of the transplanted mice. Furthermore, no recipient mouse manifested any anatomical or symptomatic evidence of leukemias, lymphomas or myeloproliferative neoplasm (MPN): lymphadenopathy, splenomegaly/organomegaly, illness or hemorrhage. Circulating $hCD45^+$ cells in PB displayed no evidence of lympho/myeloproliferation or dysplasia. Furthermore, microscopic architecture of BM, spleen and liver was normal and without fibrotic remodeling or aberrant deposition of collagen or desmin.

All images are acquired at 60x magnification. Top rows of images for each organ are secondary transplants; bottom rows of images for each organ are controls.

B. Comparative genomic hybridization analysis (CGH) shows that rEC-hMPPs are genetically stable both *in vitro* and *in vivo*. Genomic DNA was extracted from HUVECs, $CD45^+$rEC-hMPPs (35 days post-transduction) or in $CD45^+CD34^+$rEC-hMPP sorted from the engrafted NSG BM (24-weeks post-transplantation) and expanded for 72 hours *in vitro*. A human tumor sample was used as positive control of chromosome rearrangement. Extracted DNA was digested, labeled by random priming and hybridized to the Agilent 1M CGH arrays. The arrays were scanned in an Agilent DNA microarray scanner and obtained data was visualized using Feature Extraction software (version 10.7; Agilent). No genomic abnormalities were identified in $CD45^+$rEC-hMPPs (or in $CD45^+CD34^+$rEC-hMPPs engrafted in NSG BM. Hence, rEC-hMPPs remain genetically stable *in vitro* and *in vivo* and are not transformed.

Acknowledgements

V.M.S. is supported by Empire State Stem Cell Board (ESSCB) and New York State Department of Health (NYSDH: C026878). S.R. is supported by Ansary Stem Cell Institute (ASCI), HHMI, ESSCB/NYSDH: C024180, C026438, C026878, C028117, NHLBI:R01HL097797, R01HL119872,U01 HL099997NIDDK:R01DK095039,NCI:U54CA163167, Qatar National Priorities Research Foundation grant NPRP08-663-3-140 and the Qatar Foundation BioMedical Research Program. J.M.S. is suppored by grants from NCI:CA159175 and CA163167, NHLBI: HL119872 and HL055748, Starr Foundation and a Leukemia & Lymphoma Society Scholar award. J.M.B. is supported by, American Society of Hematology Scholar Award, NHLBI U01-HL099997 and Angiocrine Bioscience and ASCI. We acknowledge keycontribution of Dr. Jenny Z. Xiang for enabling and executing molecular profiling and Eric Gars for superb technical support. We appreciate Dr. William Schachterle for invaluable recommendations and edits of the manuscript.

References

1. Rafii S, et al. Human ESC-derived hemogenic endothelial cells undergo distinct waves of endothelial to hematopoietic transition. Blood. 2013; 121:770–780. [PubMed: 23169780]
2. Sturgeon CM, Ditadi A, Clarke RL, Keller G. Defining the path to hematopoietic stem cells. Nat Biotechnol. 2013; 31:416–418. [PubMed: 23657396]
3. Choi KD, et al. Identification of the hemogenic endothelial progenitor and its direct precursor in human pluripotent stem cell differentiation cultures. Cell reports. 2012; 2:553–567. [PubMed: 22981233]
4. Pereira CF, et al. Induction of a hemogenic program in mouse fibroblasts. Cell Stem Cell. 2013; 13:205–218. [PubMed: 23770078]
5. Szabo E, et al. Direct conversion of human fibroblasts to multilineage blood progenitors. Nature. 2010; 468:521–526. [PubMed: 21057492]
6. Xie H, Ye M, Feng R, Graf T. Stepwise reprogramming of B cells into macrophages. Cell. 2004; 117:663–676. [PubMed: 15163413]

7. Sandler VM, Lailler N, Bouhassira EE. Reprogramming of embryonic human fibroblasts into fetal hematopoietic progenitors by fusion with human fetal liver CD34+ cells. PLoS One. 2011; 6:e18265. [PubMed: 21533226]
8. Nolan DJ, et al. Molecular signatures of tissue-specific microvascular endothelial cell heterogeneity in organ maintenance and regeneration. Dev Cell. 2013; 26:204–219. [PubMed: 23871589]
9. Ding BS, et al. Inductive angiocrine signals from sinusoidal endothelium are required for liver regeneration. Nature. 2010; 468:310–315. [PubMed: 21068842]
10. Ding BS, et al. Endothelial-derived angiocrine signals induce and sustain regenerative lung alveolarization. Cell. 2011; 147:539–553. [PubMed: 22036563]
11. Butler JM, et al. Endothelial cells are essential for the self-renewal and repopulation of Notch-dependent hematopoietic stem cells. Cell Stem Cell. 2010; 6:251–264. [PubMed: 20207228]
12. Butler JM, et al. Development of a vascular niche platform for expansion of repopulating human cord blood stem and progenitor cells. Blood. 2012; 120:1344–1347. [PubMed: 22709690]
13. Hooper AT, et al. Engraftment and reconstitution of hematopoiesis is dependent on VEGFR2-mediated regeneration of sinusoidal endothelial cells. Cell Stem Cell. 2009; 4:263–274. [PubMed: 19265665]
14. Kobayashi H, et al. Angiocrine factors from Akt-activated endothelial cells balance self-renewal and differentiation of haematopoietic stem cells. Nature cell biology. 2010; 12:1046–1056. [PubMed: 20972423]
15. Poulos MG, et al. Endothelial jagged-1 is necessary for homeostatic and regenerative hematopoiesis. Cell reports. 2013; 4:1022–1034. [PubMed: 24012753]
16. Avecilla ST, et al. Chemokine-mediated interaction of hematopoietic progenitors with the bone marrow vascular niche is required for thrombopoiesis. Nat Med. 2004; 10:64–71. [PubMed: 14702636]
17. Ding L, Saunders TL, Enikolopov G, Morrison SJ. Endothelial and perivascular cells maintain haematopoietic stem cells. Nature. 2012; 481:457–462. [PubMed: 22281595]
18. Doan PL, et al. Tie2(+) bone marrow endothelial cells regulate hematopoietic stem cell regeneration following radiation injury. Stem Cells. 2013; 31:327–337. [PubMed: 23132593]
19. Orkin SH, Zon LI. Hematopoiesis: an evolving paradigm for stem cell biology. Cell. 2008; 132:631–644. [PubMed: 18295580]
20. Medvinsky A, Dzierzak E. Definitive hematopoiesis is autonomously initiated by the AGM region. Cell. 1996; 86:897–906. [PubMed: 8808625]
21. North TE, et al. Runx1 expression marks long-term repopulating hematopoietic stem cells in the midgestation mouse embryo. Immunity. 2002; 16:661–672. [PubMed: 12049718]
22. Yoshimoto M, Porayette P, Yoder MC. Overcoming obstacles in the search for the site of hematopoietic stem cell emergence. Cell Stem Cell. 2008; 3:583–586. [PubMed: 19041773]
23. Eilken HM, Nishikawa S, Schroeder T. Continuous single-cell imaging of blood generation from haemogenic endothelium. Nature. 2009; 457:896–900. [PubMed: 19212410]
24. Swiers G, et al. Early dynamic fate changes in haemogenic endothelium characterized at the single-cell level. Nature communications. 2013; 4:2924.
25. Rhodes KE, et al. The emergence of hematopoietic stem cells is initiated in the placental vasculature in the absence of circulation. Cell Stem Cell. 2008; 2:252–263. [PubMed: 18371450]
26. Gordon-Keylock S, Sobiesiak M, Rybtsov S, Moore K, Medvinsky A. Mouse extraembryonic arterial vessels harbor precursors capable of maturing into definitive HSCs. Blood. 2013; 122:2338–2345. [PubMed: 23863896]
27. Zovein AC, et al. Fate tracing reveals the endothelial origin of hematopoietic stem cells. Cell Stem Cell. 2008; 3:625–636. [PubMed: 19041779]
28. Chen MJ, et al. Erythroid/myeloid progenitors and hematopoietic stem cells originate from distinct populations of endothelial cells. Cell Stem Cell. 2011; 9:541–552. [PubMed: 22136929]
29. Lancrin C, et al. GFI1 and GFI1B control the loss of endothelial identity of hemogenic endothelium during hematopoietic commitment. Blood. 2012; 120:314–322. [PubMed: 22668850]
30. Hock H, et al. Gfi-1 restricts proliferation and preserves functional integrity of haematopoietic stem cells. Nature. 2004; 431:1002–1007. [PubMed: 15457180]

31. Seandel M, et al. Generation of a functional and durable vascular niche by the adenoviral E4ORF1 gene. Proc Natl Acad Sci U S A. 2008; 105:19288–19293. [PubMed: 19036927]
32. Rafii S, et al. Isolation and characterization of human bone marrow microvascular endothelial cells: hematopoietic progenitor cell adhesion. Blood. 1994; 84:10–19. [PubMed: 7517203]
33. Rafii S, et al. Human bone marrow microvascular endothelial cells support long-term proliferation and differentiation of myeloid and megakaryocytic progenitors. Blood. 1995; 86:3353–3363. [PubMed: 7579438]
34. Wu X, Lensch MW, Wylie-Sears J, Daley GQ, Bischoff J. Hemogenic endothelial progenitor cells isolated from human umbilical cord blood. Stem Cells. 2007; 25:2770–2776. [PubMed: 17641248]
35. James D, et al. Expansion and maintenance of human embryonic stem cell-derived endothelial cells by TGFbeta inhibition is Id1 dependent. Nat Biotechnol. 2010; 28:161–166. [PubMed: 20081865]
36. Ginsberg M, et al. Efficient Direct Reprogramming of Mature Amniotic Cells into Endothelial Cells by ETS Factors and TGFbeta Suppression. Cell. 2012; 151:559–575. [PubMed: 23084400]
37. Chao MP, Seita J, Weissman IL. Establishment of a normal hematopoietic and leukemia stem cell hierarchy. Cold Spring Harb Symp Quant Biol. 2008; 73:439–449. [PubMed: 19022770]
38. Notta F, et al. Isolation of single human hematopoietic stem cells capable of long-term multilineage engraftment. Science. 2011; 333:218–221. [PubMed: 21737740]
39. Zou GM, Chen JJ, Yoder MC, Wu W, Rowley JD. Knockdown of Pu.1 by small interfering RNA in CD34+ embryoid body cells derived from mouse ES cells turns cell fate determination to pro-B cells. Proc Natl Acad Sci U S A. 2005; 102:13236–13241. [PubMed: 16141339]
40. Pongubala JM, et al. Transcription factor EBF restricts alternative lineage options and promotes B cell fate commitment independently of Pax5. Nat Immunol. 2008; 9:203–215. [PubMed: 18176567]
41. Ledran MH, et al. Efficient hematopoietic differentiation of human embryonic stem cells on stromal cells derived from hematopoietic niches. Cell Stem Cell. 2008; 3:85–98. [PubMed: 18593561]
42. Doulatov S, et al. Induction of multipotential hematopoietic progenitors from human pluripotent stem cells via respecification of lineage-restricted precursors. Cell Stem Cell. 2013; 13:459–470. [PubMed: 24094326]
43. Marcelo KL, et al. Hemogenic endothelial cell specification requires c-Kit, Notch signaling, and p27-mediated cell-cycle control. Dev Cell. 2013; 27:504–515. [PubMed: 24331925]

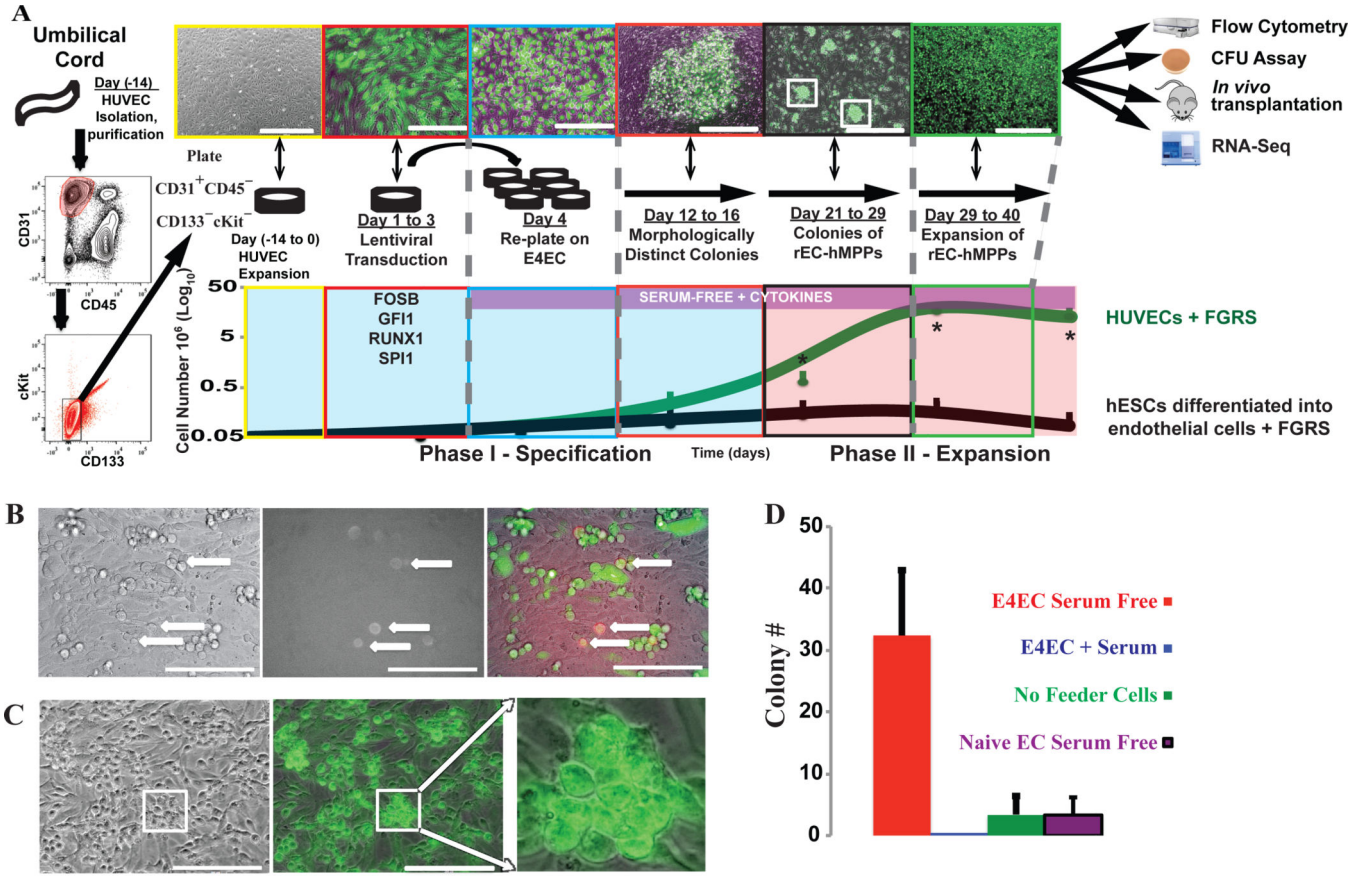

Figure 1. Reprogramming of HUVECs and hES-ECs into hematopoietic cells by FGRS TFs-transduction and vascular-induction

A. Schema of reprogramming platform of HUVECs into hematopoietic cells. $CD45^{-}CD31^{+}CD133^{-}cKit^{-}$ cells were sorted from freshly purified HUVECs and expanded (days −14 to 0). Sorted cells were transduced with FGRS (FGRS-ECs)(days 1–3) and grown in EC-media. On day 4, transduced cells were replated on E4ECs in serum-free hematopoietic media (days 12–40). Distinct GFP^{+} flat colonies were observed at days 12–16, which by days 21–29 remodeled into three-dimensional grape-like colonies. After a month (days 29–40) GFP^{+} cells expanded ~400-fold (n=4). $CD144^{+}VEGFR2^{+}$ECs derived from hES-ECs[35] were also transduced with FGRS. The process of reprogramming is subdivided into two phases: Phase I–Specification (Day 1–20) and Phase II–Expansion (Day 21–40). The expanding cultures were assayed for morphological change, cell number, and CD45. Kinetics of reprogramming of HUVECs (Green trace) and expansion of reprogrammed hES-ECs cells (Black trace).

B. Emergence of rounded hematopoietic-like $GFP^{+}CD45^{+}$ cells two to three weeks after HUVECs were transduced with FGRS (white arrows).

C. Formation of GFP^{+} hematopoietic-like colonies on the E4ECs 3–4 weeks after FGRS transduction.

D. Generation of $GFP^{+}CD45^{+}$ hematopoietic-like colonies (C) from FGRS-ECs is enhanced by co-culturing with serum-free E4ECs and blocked by presence of serum (n=8, $p<0.05$). Scale bar: 200 μm.

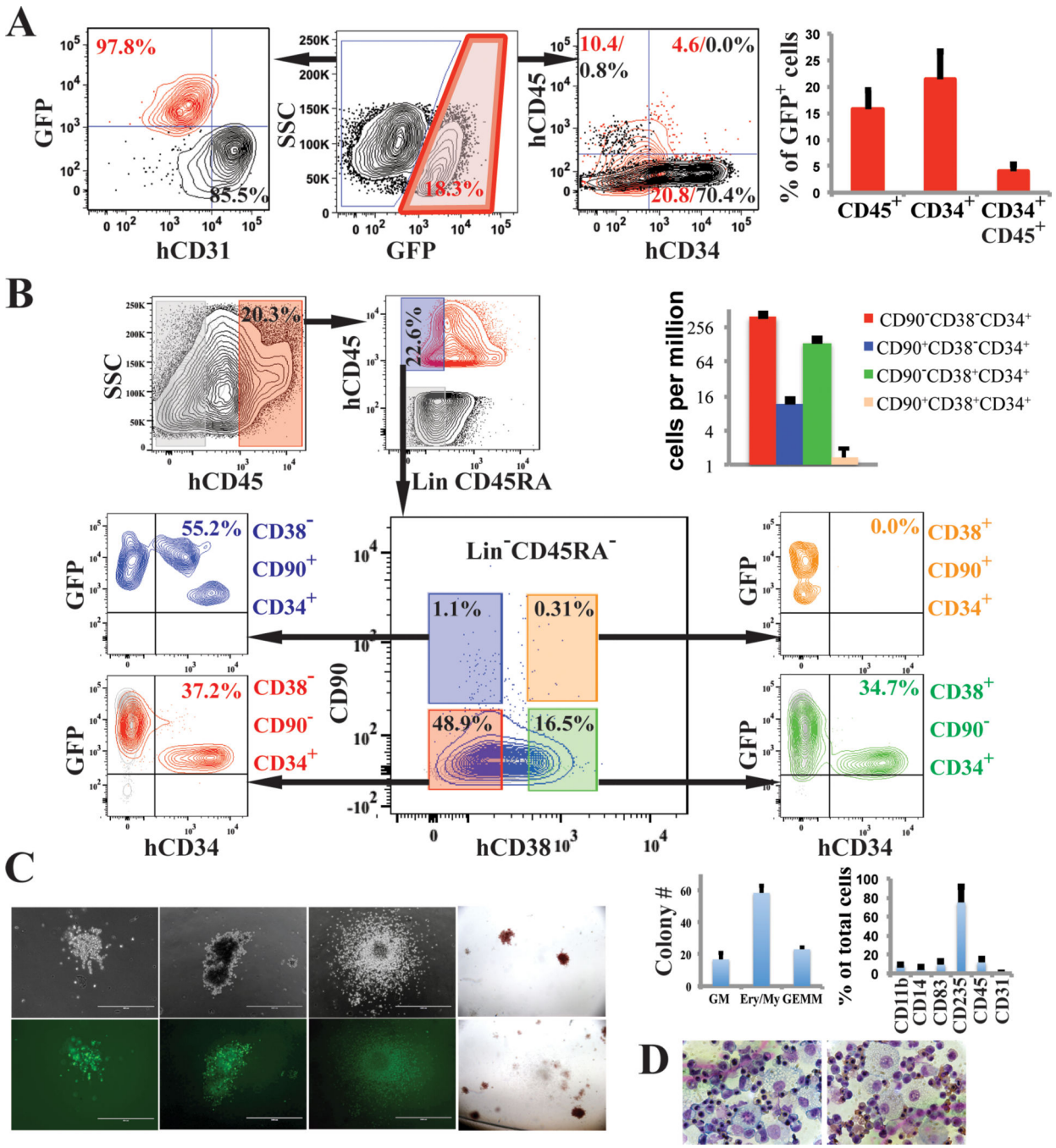

Figure 2. rEC-hMPPs phenotypically and functionally resemble multilineage HSPCs

A. FACS analysis of cocultured GFP^{-}E4ECs vascular niche along with GFP^{+} FGRS transduced HUVECs (FGRS-ECs) four weeks post-transduction (n=9).

B. Immunophenotypic analysis of FGRS reprogrammed HUVECs (red and blue; n=3).

C. Four weeks after FGRS-transduction and E4EC-induction, human GFP^{+}CD45^{+}CD34^{+} cells were sorted and seeded for CFC assay (n=3). Hematopoietic colonies arose in the CFC assay (magnificationx4); wide field (upper row) and corresponding fluorescent images (bottom row). Left to right: granulocytic-erythroid-monocytic-megakaryocytic (GEMM),

Erythroid/Myeloid, and granulocytic-macrophage (GM) colonies, and hemoglobinized colonies. Graph shows CFC assay quantification.

D. Wright-Giemsa stain of cells obtained from the CFC assay colonies. 60x magnification.

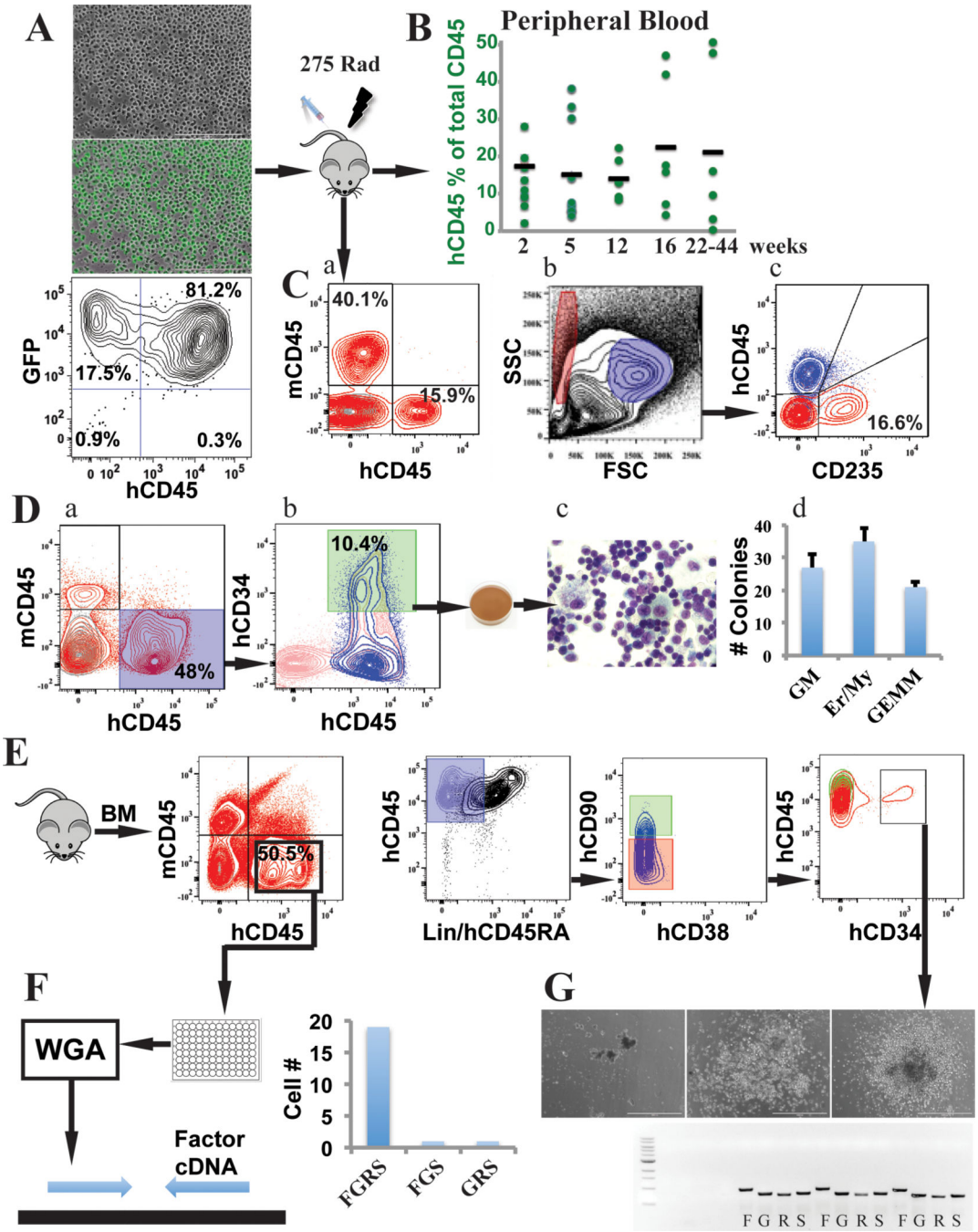

Figure 3. rEC-hMPPs are capable of *in vivo* erythro-myeloid-megakaryocytic multilineage engraftment

A. Reprogrammed HUVECs into rEC-hMPPs were transplanted into sub-lethally irradiated (275 Rad) mice (n=9).

B. Circulating human CD45^{+} (hCD45^{+}) cells were detected at 2 (n=7; 17.38±7.73%), 5 (n=6; 15.1±13.39%), 12 (n=6; 14.14±5.44%), 16 (n=6; 22.36±17.95%) and 22 to 44 (22–44) (n=6; 21.23±22.27%) weeks post transplantation. The 22–44 weeks engrafted mice were

used for further analyses of the myelodysplasia and fibrotic changes (Extended Data Figure 8,9,10A).

C. Analysis of the total mononuclear peripheral blood cells at 16 weeks post-transplantation of $hCD45^+$and mouse $CD45^+$($mCD45^+$) cells, revealed presence of $hCD45^+$(15 9%) and human non-erythroid circulating cells (a). We gated on the FSC/SSC $hCD45^-$ erythroid compartment (Red gate) and typical human non-erythroid $hCD45^+$ compartment (Blue gate) (b,c).

D. rEC-hMPPs isolated from the host retained their multilineage potential in vitro; secondary CFC-assay. Engraftment of mouse bone marrow (BM) 22 weeks post-transplantation is shown (a). The cells were expanded *in vitro* for 24 hours (b) and FACS resorted for $hCD45^+hCD34^+$ cells for CFC assay. Wright-Giemsa stain (c) of the cytospin of the cells from CFC assay, (magnificationx100 right). Quantification of the CFC assay (d).

E. Phenotypic analysis of an *in vivo* 22 weeks engrafted rEC-hMPPs in BM shows human $CD45^+Lin^-$ $CD45RA^-CD38^-CD90^-CD34^+$ MPPs.

F. Identification of viral integration on a single-cell level. Whole genome amplification (WGA) of 21 $hCD45^+$cells isolated from a host mouse (E). Quantification of the analysis is shown in the right graph.

G. Identification of viral integration on a single-colony level. $Lin^-CD45RA^-CD38^-CD90^-$ $CD34^+$cells (10 cells) were used for a CFC assay. We detected all four FGRS viral vectors in all CFC colonies tested (bottom image; Letters *FOSB* (F), *GFI1* (G), *RUNX1* (R), *SPI1* (S) show PCR products specific for each of these factors in the first colony).

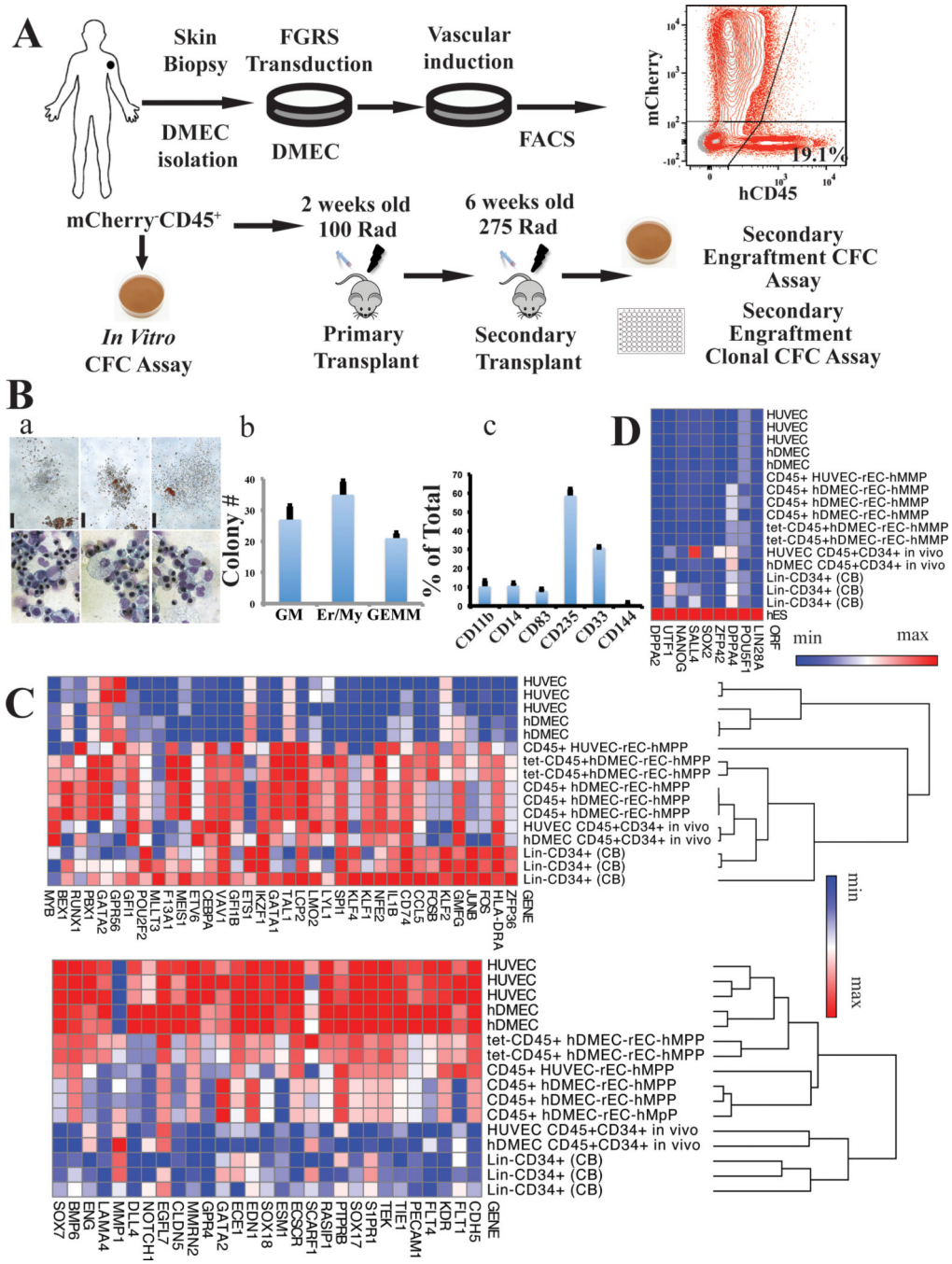

Figure 4. Functional and transcriptional analysis of adult hDMEC-derived rEC-hMPPs

A. Schematic representation of *in vitro* and *in vivo* functional tests of hDMEC-derived rEC-hMPPs. **B**. (a) Hematopoietic colonies observed in CFC assay (scale bar: 200μm); wide field (upper row). Wright-Giemsa stain of cells from CFC colonies (magnification x60) (bottom row). (b) Quantification of the CFC assay(n=3). (c) Immunophenotypic quantification of surface marker expression in CFU colonies(n=3).

C. Global gene transcription profiling of *in vitro* generated $CD45^+$ rEC-hMPPs (derived from hDMEC and HUVECs) and *in vivo* engrafted HUVEC-derived $CD45^+CD34^+$rEC-

hMPPs, 22 weeks post-transplantation and hDMEC-derived $CD45^+CD34^+$rEC-hMPPs, 15 weeks post-secondary engraftment (4A). EC-endothelial cells, CB–cord blood cells.
D. Comparison of expression of prototypical pluripotency genes shown in (4C). Human embryonic stem cells (hES). The data in C and D are presented as $\log_2$ (transcription level).

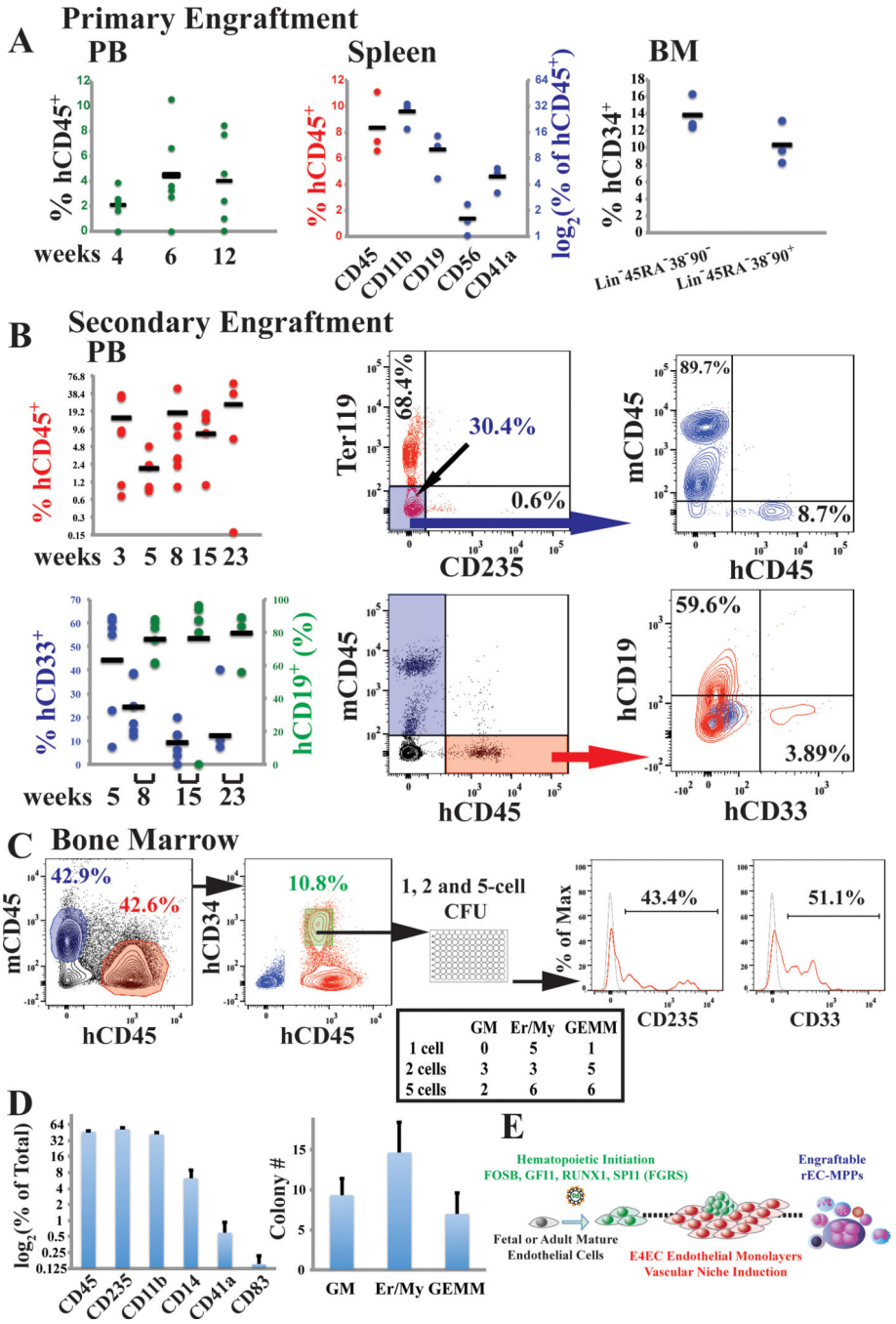

Figure 5. Adult human hDMECs-derived rEC-hMPPs are capable of *in vivo* primary and secondary multilineage engraftment

A. Analysis of PB of mice at 4, 6, and 12 weeks post-primary transplantation(n=6). Analysis of spleen and BM of mice at 14 weeks post-primary transplantation(n=3).

B. Analysis of the PB of mice at 3, 5, 8 (n=6), 15 (n=4) and 23 (n=4) weeks post-secondary transplantation (n=6). FACS plots on the right show representative analysis of rEC-hMPP secondary engraftment. Mouse Ter119^{+} and human CD235^{+} erythroid populations were excluded to obtain an accurate estimation of hCD45^{+} and mCD45^{+}cells.

C. Clonal CFC assay of BM hCD45^{+}hCD34^{+}cells(n=3; left plot). Emerging colonies were counted and classified (middle table). CFC colonies derived from single plated hCD45^{+}hCD34^{+} cell comprise of mixed-lineage erythroid and myeloid progenies(right plots).

D. Reprogrammed cells isolated from the host retained their multi-lineage potential *in vitro*; secondary CFC assay.

E. Schematic representation of steps of reprogramming of ECs into rEC-hMPP by FGRS.